CHAPTER 4
CONSTITUTIVE MODELING FOR SOIL-BENTONITE

4.1 Introduction

Constitutive models can be used to describe the stress-strain behavior of soils. They can provide a framework for understanding how soil will behave under different loading conditions, and they can be implemented in finite element and finite difference codes for use in numerical analyses. In complex loading conditions, such as the consolidation of soil-bentonite backfill in a cutoff wall, a constitutive model is necessary to make numerical predictions of how the soil-bentonite will deform and transfer stress. There are many published constitutive models in the literature of varying levels of complexity.

This chapter describes the procedures used to evaluate existing constitutive models and to develop a constitutive model that provides a good representation of soil-bentonite behavior. Published literature was reviewed to identify important aspects of choosing a constitutive model and to identify constitutive models that would be applicable to soil-bentonite. This review process started with the following models that are relatively simple and frequently used: the hyperbolic model (Duncan and Chang 1970), Modified Cam Clay model (Roscoe and Burland 1968), and Cam Clay model (Roscoe and Schofield 1963). The extensive laboratory testing program performed on soil-bentonite mixture SB1 provided the stress-strain data to evaluate the constitutive models. The model parameter values for SB1 were obtained for each of the models. The models were then evaluated to determine how well they match the laboratory test data. The models provided a good prediction of the behavior of soil-bentonite for some tests but poor predictions in other tests. Two other models that are special cases of a more complicated model by Kutter and Sathialingam (1992) were then evaluated. These models are Modified Cam Clay type models and are referred to here as the R model and the RS model.

Of all the constitutive models evaluated, it was found that the RS model provides the best representation of the behavior of soil-bentonite mixture SB1. The RS model provides a good match of the stress-strain behavior of SB1 in all the laboratory tests. The RS model was then applied to the tests performed on SB3. It was found that the RS model also provides a reasonable representation of the stress-strain behavior of SB3.

In this chapter, information from the literature on selecting a constitutive model is presented first. Next constitutive models are evaluated in the following order: hyperbolic model, Modified Cam Clay model, Cam Clay model, R model, and RS model. For each model, a description of the model is given, the model parameters for SB1 are evaluated, a comparison of the model with laboratory tests performed on SB1 is presented, and the model is evaluated for its application to soil-bentonite. In the process of evaluating the constitutive models, the shape of the yield surface and the shape of the plastic potential surface for SB1 were determined. The method for determining the surfaces and the results are presented. Finally, the RS model is compared with various laboratory tests performed on SB3.

4.2 Important Aspects of Selecting a Constitutive Model

In selecting a constitutive model for soil, Wood (1990) suggests considering the past and future history of the soil and identifying an appropriate level of complexity. He suggests that for engineering purposes, a relatively simple model like the Modified Cam Clay model can be modified and levels of complexity added as necessary in order to provide insight into particular problems. Wroth and Houlsby (1985) suggest that in order for a constitutive model to be useful in solving engineering problems, it should be simple and reflect the physical behavior of the soil. Duncan (1994) states that for constitutive models to be practical, it should be possible to obtain the model parameters values in a simple manner from conventional soil tests.

Duncan (1994) states that simple elasticity models, such as the hyperbolic model, can be applied for stable structures where deformations are small, orientation of stresses are constant, and for fully drained or completely undrained conditions. For accurate predictions of stress-strain behavior near failure and for undrained pore pressures due to application of total stress external loads, Duncan (1994) states that more complex elastic-plastic models, such as the Cam Clay model, should be used.

Duncan (1994) reviewed almost 2000 papers related to geotechnical applications of constitutive models or finite element modeling. Of these papers, he states that commonly used models are the hyperbolic model (Duncan and Chang 1970), Modified Cam Clay model (Roscoe and Burland 1968), and versions of the Cam Clay model.

4.3 Evaluation of Hyperbolic Model for Soil-Bentonite

The hyperbolic model described by Duncan and Chang (1970) is a nonlinear elastic constitutive model. The model is simple and commonly used. Although soils are inelastic, the model can simulate several important aspects of realistic soil behavior. By using a Young's modulus that is a function of stress level and confining pressure, and a bulk modulus that is a function of confining pressure, the model can simulate nonlinear stress-strain and stress dependency. By using a different Young's modulus for loading and unloading, the model can simulate inelastic behavior (Duncan et al. 1980). A brief summary of the description given by Duncan et al. (1980) is presented here.

The model uses a hyperbolic curve to represent the stress-strain curve for a soil. The hyperbola is given by the following equation:

$$(\sigma_1 - \sigma_3) = \frac{\varepsilon}{\frac{1}{E_i} + \frac{\varepsilon}{(\sigma_1 - \sigma_3)_{ult}}} \qquad (4.1)$$

where: ε = axial strain

E_i = initial slope of the stress-strain curve

$(\sigma_1-\sigma_3)_{ult}$ = the asymptotic value that the hyperbola approaches

E_i is related to the confining pressure by:

$$E_i = KPa\left(\frac{\sigma_3}{Pa}\right)^n \tag{4.2}$$

where K is the modulus number, n is the modulus exponent, and Pa is atmospheric pressure. $(\sigma_1-\sigma_3)_{ult}$ can be related to the strength of the soil by the following equation:

$$R_f(\sigma_1-\sigma_3)_{ult} = (\sigma_1-\sigma_3)_f \tag{4.3}$$

where R_f is the failure ratio and $(\sigma_1-\sigma_3)_f$ is the strength of the soil. The strength of the soil can be expressed in terms of the Mohr-Coulomb failure criterion by the following:

$$(\sigma_1-\sigma_3)_f = \frac{2c'\cos\phi' + 2\sigma'_3\sin\phi'}{1-\sin\phi'} \tag{4.4}$$

The current stress state can be defined by the stress level, SL, given by:

$$SL = \frac{(\sigma_1-\sigma_3)}{(\sigma_1-\sigma_3)_f} \tag{4.5}$$

The above equations can be combined to produce the following equation for the tangent Young's modulus, E_t:

$$E_t = E_i(1-R_f SL)^2 \tag{4.6}$$

For unloading and reloading, the model uses a different Young's modulus, E_{ur}, that is related to confining pressure by:

$$E_{ur} = K_{ur}Pa\left(\frac{\sigma_3}{Pa}\right)^n \tag{4.7}$$

where the only new parameter is K_{ur} which is the unloading-reloading modulus number.

The volume change characteristics are defined by a bulk modulus, B, that is related to confining pressure by:

$$B = K_b Pa\left(\frac{\sigma_3}{Pa}\right)^m \tag{4.8}$$

where K_b is the bulk modulus number and m is the bulk modulus exponent.

Evaluation of Model Parameters for SB1

The parameter values for SB1 were found by applying the procedure described in Duncan et al. (1980) using the results of three normally consolidated CD tests (CD_1, CD_8, and CD_10). The strength values of $\phi' = 32°$ and $c' = 0$ were used based on the results of eight CU tests and five CD tests performed on SB1 presented in Chapter 3. The graphs used to find the parameter values for the hyperbolic model are shown in Figure 4.1. The resulting parameter values are listed in Table 4.1 in the row labeled "CD tests".

The parameter values for SB1 were also found using the procedure described in Clough and Duncan (1969) using one-dimensional consolidation tests. This was done because often times CD test data is unavailable in practice. For this method, stress-strain curves from two one-dimensional consolidation tests (tests C5 and C6) were used to estimate the values of the parameters K, n, K_b, and m. A friction angle of $\phi' = 32°$ was used. The value of R_f was estimated based on values given in Table 5 of Duncan et al. (1980) for silty clayey sands similar to SB1. A value of K_o is necessary to obtain model parameters from 1-D consolidation tests. K_o was estimated from correlations rather than from the K_o tests described in Chapter 3 because K_o tests results are not normally available in practice.

The value of K_o was estimated by averaging values from three sources:

1. Data from many soils with measured K_o values compiled by Mayne and Kulhawy (1982). Soils with Atterberg limits similar to SB1 (LL=34, PI=18) were averaged. Estimated K_o=0.46.

2. Brooker and Ireland (1965) graph of K_o versus plasticity index. For a normally consolidated clay with plasticity index=18, estimated $K_o = 0.53$.
3. Jaky (1948) correlation for sands K_o=1-sin ϕ'. For ϕ=32°, estimated K_o=0.47.

An average value of K_o=0.49 was used. The parameter values using the Clough and Duncan (1969) procedure are also given in Table 4.1 under the row labeled "1-D consolidation tests."

Table 4.1 Hyperbolic Parameter Values for SB1

Parameter Values Found From:	c' (psi)	ϕ' (degrees)	K	n	Pa (psi)	R_f	K_b	m
CD Tests	0	32	31.4	1.23	14.7	0.61	11.9	1.12
1-D Consolidation Tests	0	32	70.0	0.88	14.7	0.67	25.3	0.86

Stark and Vettel (1991) also compared the hyperbolic parameter values determined from CD tests and consolidation tests. They tested a "slopewash" material with index properties similar to SB1 (slopewash: LL=40, PL=20, OCR=1 to 1.5, CL classification; SB1: LL=34, PL=16, OCR=1, SC classification). For normally consolidated soils with similar index properties to the slopewash, Stark and Vettel recommend finding the modulus numbers K and K_b from consolidation tests and scaling them up by factors of 1.9 and 3.2 respectively to get triaxial modulus numbers. Although the index properties are similar, the opposite trend was found for SB1. The modulus numbers K and K_b are larger using the consolidation tests than the CD tests.

Comparison of Hyperbolic Model with Laboratory Tests on SB1

The hyperbolic model (with the two sets of parameter values) was used to model the three CD tests on SB1. The results are shown in Figure 4.2. As expected, the hyperbolic model parameters that were found from the CD tests provide a good fit to the CD test data. The hyperbolic model parameters that were found from the consolidation tests do not provide

a good fit. At all three confining pressures, the parameter values from the consolidation tests produce a much stiffer stress-strain response than measured, and the volumetric strain data is very significantly underpredicted.

The hyperbolic model (with the two sets of parameter values) was used to model the 1-D consolidation test C5. The results are shown in Figure 4.3. A spreadsheet program developed by David Bentler was used for this analysis. As expected, the model gives a good fit using the parameters found from the consolidation tests. The model gives a poor fit using the parameters found from the CD tests. The value of K_o calculated by the spreadsheet program for both sets of parameter values ranges from K_o=0.47 to 0.5.

Hyperbolic Model Summary

The hyperbolic model gives good predictions of the tests that were used to determine the parameter values, but it does not give good predictions of other stress conditions. The model also has other limitations, as discussed in Duncan (1994), that limit its applicability to model soil-bentonite in cutoff wall applications. The hyperbolic model cannot accurately predict pore pressure generation and dissipation during coupled consolidation analysis, and may not give accurate results for the complex loading conditions in a soil-bentonite cutoff wall.

4.4 Evaluation of Cam-Clay Model and Modified Cam Clay Model for Soil-Bentonite

The Cam Clay model was first presented in the literature in 1963 (Roscoe and Schofield 1963). Later, a revised version called the Modified Cam Clay was introduced (Roscoe and Burland 1968). Both models are elastic-plastic models based on the critical state concept. The Modified Cam Clay model has been more widely used in practice than the Cam Clay model (Wood 1990).

State variables associated with the cam clay models and the rest of the models in this chapter are given below:

p' = general volumetric effective stress

= mean effective stress, $(\sigma'_a+2\sigma'_r)/3$ (for triaxial conditions)

q = general deviator stress

= deviator stress, $(\sigma'_a-\sigma'_r)$ (for triaxial conditions)

η = q/p'

e = void ratio

v = specific volume = 1 + e

where σ'_a = effective axial stress and σ'_r = effective radial stress.

Model parameters for the cam clay models are given below:

λ = slope of the isotropic normal compression line

κ = slope of the isotropic unload-reload line

M = critical state parameter

ν' = Poisson's ratio

G = shear modulus

The same choice of symbols for strain that is used by Wood (1990) is adopted here and is summarized below:

ε_p = general volumetric strain

= $\varepsilon_a+2\varepsilon_r$ (for triaxial conditions)

ε_q = general deviatoric strain

= triaxial shear strain, $\frac{2}{3}(\varepsilon_a - \varepsilon_r)$ (for triaxial conditions)

where ε_a = axial strain and ε_r = radial strain. Since most of the laboratory testing presented in Chapter 3 was under triaxial conditions, ε_q will be referred to as the triaxial shear strain (shear strain). This is the same convention used by Wood (1990) and also Gens and

Potts (1988). Note that for triaxial conditions, ε_q can be thought of as the deviatoric component of the axial strain.

The volumetric strain is made up of elastic volumetric strain and plastic volumetric strain. The shear strain is made up of elastic shear strain and plastic shear strain as follows:

$$\varepsilon_p = \varepsilon_p^e + \varepsilon_p^p \tag{4.9}$$

$$\varepsilon_q = \varepsilon_q^e + \varepsilon_q^p \tag{4.10}$$

where ε_p^e = elastic volumetric strain

ε_p^p = plastic volumetric strain

ε_q^e = elastic shear strain

ε_q^p = plastic shear strain

Elastic-plastic models have the following components: elastic properties, yield surface, plastic potential, and hardening rule (Wood 1990). Essential components of the cam clay models are illustrated in Figure 4.4. The unload-reload line (url) and the isotropic normal compression line (icl) describe the soil's compressibility and are assumed to be linear in the graph of ln p' versus specific volume. The slope of the unload-reload line is kappa, κ, and the slope of the isotropic normal consolidation line is lambda, λ. The critical state line is parallel to the isotropic normal compression line. At the critical state line, "*unlimited plastic shear strains develop without plastic volumetric strain*," (Wood 1990). The parameter N determines the location of the compression curve in the stress-strain space. N is the value of specific volume on the isotropic normal consolidation line at a value of p'=1. The parameter Γ is the value of specific volume on the critical state line at a value of p'=1. The values of N and Γ are dependent on the units used.

For the Cam Clay model, the elastic volumetric strain and the elastic shear strain increments can be expressed by the following equations:

$$\delta\varepsilon_p^e = \frac{\kappa}{vp'}\delta p' \tag{4.11}$$

$$\delta\varepsilon_q^e = 0 \tag{4.12}$$

where v is the specific volume of an initial state from which strains are measured and p' is the mean effective stress at the beginning of the stress increment.

For the Modified Cam Clay model, the elastic volumetric strain and the elastic shear strain increments are given by the following equations:

$$\delta\varepsilon_p^e = \frac{\kappa}{vp'}\delta p' \tag{4.11}$$

$$\delta\varepsilon_q^e = \frac{1}{3G}\delta q \tag{4.13}$$

where G is the shear modulus. The volumetric strain can also be expressed in terms of the bulk modulus, K. The definition of the bulk modulus is:

$$K = \frac{\delta p'}{\delta\varepsilon_p^e} \tag{4.14}$$

For both cam clay models, the bulk modulus is equal to:

$$K = \frac{vp'}{\kappa} \tag{4.15}$$

The yield function, f, determines the boundary between purely elastic and elastic-plastic deformation. At stress states below the yield surface, only elastic deformation occurs. At the yield surface, elastic and plastic deformation occurs. The yield function for the Cam Clay model is given by the following equation (Britto and Gunn 1987):

$$f = q - Mp'\ln\frac{p_c'}{p'} = 0 \tag{4.16}$$

where M is the slope of the critical state line in p-q space. The hardening parameter, p_c', controls the size of the yield surface. The shape of the yield function for the Cam Clay model is a bullet shape. The yield function for the Modified Cam Clay model is given by the following equation (Wood 1990):

$$f = q^2 - M^2 p'(p_o' - p') = 0 \tag{4.17}$$

where p_o' is the hardening parameter for the Modified Cam Clay model. The shape of the yield function for the Modified Cam Clay model is an ellipse. The shapes of the yield functions are shown in Figure 4.4. For the Cam Clay model, the yield surface intersects the M line at $p'_c/2.72$. For the Modified Cam Clay model, the yield surface intersects the M line at $p'_o/2$.

The plastic potential function, g, describes the relative magnitudes of the plastic shear strain and the plastic volumetric strain when the soil is yielding. Both models assume the condition of normality, meaning the plastic potential function, g, is equal to the yield function, f. The ratio of the plastic shear strain to the plastic volumetric strain is given by the direction of the plastic strain increment vector. The plastic strain increment vector is perpendicular to the plastic potential function as shown in Figure 4.4.

The magnitude of the plastic deformations and the change in the size of the yield surface is described by the hardening rule. The cam clay models assume the yield surface expands at a constant shape and the expansion is linked to the isotropic normal compression line. The hardening rule for both models can be described by the following equation (Wood 1990):

$$\delta p_o' = \frac{v p_o'}{\lambda - \kappa}\delta\varepsilon_p^p \tag{4.18}$$

where p'_o would be used for the Modified Cam Clay model and p'_c would be substituted for p'_o for the Cam Clay model.

Evaluation of Model Parameters for SB1

The values of C_c and C_r from the first isotropic consolidation test IC_1 on SB1 were used to calculate values of λ and κ. The parameters are related by the following equations:

$$C_c = 2.3\lambda \tag{4.19}$$

$$C_r = 2.3\kappa \tag{4.20}$$

The parameter values are λ=0.07 and κ=0.0048 for SB1. The compression values obtained from the second isotropic consolidation test IC_2 were not used in this calculation, since the test was run over a much smaller stress range for the purposes of defining the yield surface. The values from IC-1 are consistent with the data from IC_2.

The value of N was determined by plotting the data from isotropic consolidation test IC_1 and the isotropically consolidated CU tests, as shown in Figure 4.5. The N value is the specific volume at a mean effective stress of one. For units of psf, N is 2.044. For other units, N has different values as listed in the figure.

Assuming the soil-bentonite is isotropic, only two elastic parameters are needed to define its elastic behavior (Wood 1990). As previously stated, for the cam clay models, the bulk modulus, K, is given by:

$$K = \frac{vp'}{\kappa} \tag{4.15}$$

which indicates that the bulk modulus varies with mean effective stress p'.

The bulk modulus can be related to the Poisson's ratio, ν', and shear modulus by the following equation:

$$G = K\frac{3}{2}\frac{(1-2\nu')}{(1+\nu')} \tag{4.21}$$

If a constant shear modulus is used, equation 4.21 implies that the Poisson's ratio varies with mean effective stress, since the bulk modulus is a function of mean effective stress. Alternatively, it is possible to assume that Poisson's ratio is constant and the shear modulus is a function of mean effective stress (Wood 1990). As discussed in Gens and Potts (1988), it has been shown that the use of a variable shear modulus can result in a model that does not conserve energy. They state that this may be significant in applications with many loading cycles and stress reversals but may not be important for monatomic loading, which is the case for cutoff walls. They also state that a constant shear modulus does not agree with experimental evidence and can imply negative values of Poisson's ratio at low p'. Wroth and Houlsby (1985) state that for most soils it is reasonable to assume a constant Poisson's ratio and a variable shear modulus.

For these reasons, a constant Poisson's ratio was assumed with a shear modulus that is a function of p'. Combining equations 4.15 and 4.21, the following relationship was used to represent the shear modulus:

$$G = \frac{3(1-2\nu')vp'}{2(1+\nu')\kappa} \tag{4.22}$$

The shear modulus was determined experimentally at various consolidation pressures in order to solve for the relationship with Poisson's ratio. The shear modulus was estimated from the initial stress-strain curve of each CU test. If the shear stress, q, versus shear strain, ε_q, is plotted for a CU test, the initial slope of the curve is equal to 3G (Wood 1990). For a CU test, the shear strain is equal to the axial strain, and the stress-strain curves presented in Chapter 3 can be used to obtain values of G. For each CU test, the shear modulus is plotted versus vp' (the specific volume multiplied by the initial mean

effective stress), as shown in Figure 4.6. By finding the relationship between G/vp' from the graph, and by knowing κ, the value of Poisson's ratio can be determined from equation 4.22. For the data in Figure 4.6, the value of Poisson's ratio is 0.37.

The strength parameters were determined from the results of the CU and CD tests, which are presented in Chapter 3. The value of M is 1.3. A summary of the model parameter values determined for SB1 is shown in Table 4.2.

Table 4.2 Cam Clay and Modified Cam Clay Parameter Values for SB1

λ, lambda	κ, kappa	ν', Poisson's ratio	M	N
0.070	0.0048	0.37	1.3	2.044 for p' in psf 1.696 for p' in psi 1.834 for p' in kPa

Shape of the Yield Surface for SB1

The shape of the actual yield surface for SB1 was estimated from CD tests on overconsolidated specimens. The CD tests CD_2 through CD_7 were isotropically consolidated to 20 psi and isotropically unloaded to various overconsolidation ratios. The samples were then sheared drained in order to find the yield point. At the yield point, the compressibility and stress-strain behavior significantly changed. For each test, several plots were used in order to estimate the yield point. Stress-strain curves, specific volume, and work were plotted. The work for a triaxial test is given by (Wood 1990):

$$\text{Work} = \int (p'd\varepsilon_p + qd\varepsilon_q) \qquad (4.23)$$

where the trapezoidal rule was used to evaluate the integral. An example of the plots used to find the yield point is given in Figure 4.7 for test CD_4 which was sheared at OCR=1.1. All of the plots in Figure 4.7 for CD_4 give consistent estimates of the yield point, which was determined to be at p'=20.5 psi and q=6.0 psi.

The yield points for each test were normalized with respect to the effective mean consolidation pressure (p_{con}) and plotted in Figure 4.8. As an example, the mean effective consolidation pressure for CD_4, whose yield point is evaluated from Figure 4.7, was 20.31 psi. The normalized yield point is plotted at approximately (1.0, 0.30) on the p'/p_{con} versus q/p_{con} graph. Tests CD_2, CD_3, CD_5, CD_6, and CD_7 were sheared at overconsolidation ratios that were higher than CD_4 and the yield points from these tests lie to the left of the yield point for CD_4.

Also plotted on this graph are the yield points from CD_1, CD_8, and CD_10, which were normally consolidated. As can be seen from the stress-strain curves of CD_8 in Figure 4.9, the sample exhibits an initially stiff response. It is believed that this effect is due to secondary compression or thixotropic hardening that occurred prior to shearing. All of the samples experienced some secondary compression on the order of one half to one day. Although very little compression occurred during this time, the samples behaved as if they were consolidated to a pressure beyond the actual consolidation pressure. This phenomenon was first noticed by Leonards and Ramiah (1959) who discovered that, after periods of secondary compression, a clay was able to withstand pressures greater than the maximum past pressure with very little deformation. This pressure was called the "quasi-preconsolidation" pressure. Alternatively, the samples may have experienced a thixotropic strength increase. Regardless of the mechanism, all of the triaxial samples experienced some strength gain during the consolidation phase beyond the consolidation pressure. All of the normalized yield points for the supposedly normally consolidated CD tests are clustered around (1.08, 0.23) on the graph.

In order to further investigate aging effects on the triaxial tests, an isotropic consolidation and isotropic rebound test IC_2 was run. The sample was isotropically consolidated to 20.3 psi, isotropically rebounded to 10 psi, and isotropically reloaded in increments of 2

psi in order to find the yield point. The estimated yield point was at 22.0 psi. The normalized yield point for this test is plotted in Figure 4.8 along the p' axis at 1.08. The isotropic test IC_2 quantifies the aging effects, prior to shearing, to be approximately 8%.

The data in Figure 4.8 indicate that the shape of the yield function for SB1 is elliptical and has a different shape to the left and the right of the critical state line. The top of the yield function is very flat. The region to the left of the critical state line is largely unknown; however, this region is not of great concern for this research since it corresponds to highly overconsolidated material and the soil-bentonite in a cutoff wall should be close to normally consolidated.

Comparison of Cam Clay and Modified Cam Clay Models with Laboratory Data from SB1

The shapes of the yield functions for the Cam Clay model and the Modified Cam Clay model are compared to the shape of the yield surface estimated for SB1 in Figure 4.10. It can be seen from the figure that the shape of the yield surface for the cam clay models is not very similar to the shape of the yield surface obtained from experimental data. Wood states that although the yield surface may not be realistic for many natural soils, the differences between the simple Modified Cam Clay model and more complex models may not be important for practical applications (Wood 1990).

In order to compare the laboratory test results with the cam clay models, the normally consolidated CU and CD tests were normalized with respect to the mean effective consolidation pressure, p_{con}. The overconsolidated samples were not compared to the models since soil-bentonite placed in a cutoff wall would be normally consolidated. Since the normalized curves were all similar in shape, a representative curve was compared to the models. The normalized plots of the CU tests are shown in Figure 4.11 with the representative curve indicated by open circles. The normalized plots of CD tests are shown in Figure 4.12 with the representative curve indicated by open circles.

The normalized stress paths of the CU tests indicate that the average effective mean stress, immediately prior to shear, was 0.94 times the mean consolidation pressure. This decrease in mean effective stress was due to undrained creep mentioned in Section 3.5. The drainage valve was closed for a period of time before the piston made contact with the sample, resulting in excess pore pressures due to undrained creep. The average value of normalized excess pore pressure was used in the modeling. The average normalized initial shear stress in the sample due to the membrane correction discussed in Section 3.5 was -0.03. Since this effect is small, it was not modeled. The drainage valve was never closed for the CD tests and the excess pore pressure build up was not experienced.

Spreadsheet programs were developed to model triaxial CD and CU tests for the Cam Clay and Modified Cam Clay models. The CU and CD tests were simulated with and without accounting for aging. If aging was not modeled, the consolidation pressure was used as the preconsolidation pressure, and this is denoted as $p_o=1.0\ p_{con}$ in subsequent figures. If aging was modeled, the preconsolidation pressure used was 10% greater than the actual consolidation pressure, and this is denoted as $p_o=1.1p_{con}$. In the CU tests, undrained creep was modeled by assuming an initial excess pore pressure at the start of shear. An average value from the normalized CU tests was assumed.

The comparison of the cam clay models with the representative CU test is shown in Figure 4.13. The representative curve is shown by the solid line with the open circles. Both models over predict the undrained shear strength. The Cam Clay model is closer to the representative curve. The Modified Cam Clay model grossly over predicts the undrained shear strength. Due to the effects of the initial excess pore pressures in the specimen and aging, the models predict an initial elastic response. For the cam clay models, an elastic stress path in an undrained test is vertical until the stress path hits the yield surface (Wood 1990). After yielding, the yield surface expands and the stress path follows the shape of

the expanding yield surface. The general shape of the stress-strain curve is well matched by both models. The excess pore pressure is reasonably well predicted by the models. Again, the Cam Clay model is closer to the representative curve than the Modified Cam Clay model. It can be seen that the effect of aging is to slightly increase the undrained shear strength and to slightly decrease the excess pore pressures.

The comparison of the cam clay models with the representative CD test is shown in Figure 4.14. The representative curve is shown by the plain solid line. Only the end points of the stress paths for the models are shown. For a CD test, the stress path rises at a 3 on 1 slope until it hits the critical state line. All of the models predict the same drained strength since the same failure criterion, M, was used for all the models. The Cam Clay model matches the representative stress-strain and volumetric strain curves very well. The effect of aging is negligible on the stress-strain curve. Aging very slightly decreases the volumetric strain at a given axial strain. The Modified Cam Clay model predicts a stiffer stress-strain response than measured and significantly less volumetric strain than measured.

The comparison of the Modifed Cam Clay model with the 1-D consolidation test C5 is shown in Figure 4.15. It can be seen that the agreement is good except for the unloading portion. This is because the unloading behavior is not exactly elastic as assumed in the model. This Modified Cam Clay curve was generated by theoretically determining the η value (q/p') that corresponds to the condition of K_o loading. This value of η is designated η_{Ko}. For the condition of no lateral strain, the following relationship between volumetric and shear strain holds (Wood 1990):

$$\frac{\delta\varepsilon_p}{\delta\varepsilon_q} = \frac{3}{2} \tag{4.24}$$

This condition can be substituted into equations of elastic and plastic volumetric strain and elastic and plastic shear strain for Modified Cam Clay in order to obtain the following relationship between η_{Ko} and the model parameters (Wood 1990):

$$\frac{\eta_{Ko}(1+\nu')(1-\Lambda)}{3(1-2\nu')} + \frac{3\eta_{Ko}\Lambda}{M^2 - \eta_{Ko}^2} = 1 \tag{4.25}$$

where

$$\Lambda = \frac{\lambda - \kappa}{\lambda} \tag{4.26}$$

The parameter Λ is 0.93 for SB1. Wroth and Houlsby (1985) state that there is limited data on the value of Λ but that a typical value for clay is 0.8. Since the rebound measured for SB1 was so small, the value of Λ is much closer to one than for a typical clay.

Using the above equations with the parameter values found for SB1, η_{Ko} is 0.488 for Modified Cam Clay. For triaxial conditions, η_{Ko} is related to K_o by the following two equations (Wood 1990):

$$\eta_{Ko} = \frac{3(1-K_o)}{1+2K_o} \tag{4.27}$$

$$K_o = \frac{3-\eta_{Ko}}{3+2\eta_{Ko}} \tag{4.28}$$

The value of K_o predicted by the Modified Cam Clay model for SB1 is 0.63, which is about 11% larger than the measured value of K_o (K_o=0.57 from test Ko_2 presented in Section 3.4).

A simplified procedure by Kutter and Sathialingam (1992) was used to estimate K_o for the Cam Clay model. Neglecting the elastic strains, the following equation in terms of the plastic potential function, g, holds for the condition of zero lateral strain:

$$\frac{\delta\varepsilon_p}{\delta\varepsilon_q} = \frac{3}{2} \cong \frac{\frac{\delta g}{\delta q}}{\frac{\delta g}{\delta p}} \tag{4.29}$$

Using equation 4.29 and the expression for the plastic potential function (equation 4.16), the following relationship relating η_{Ko} and the model parameters results:

$$\eta_{Ko} = \frac{-3+2M}{2} \tag{4.30}$$

Using the parameter values for SB1, equation 4.30 predicts a negative value of η_{Ko}, which is not physically reasonable. A negative value of η for a 1-D consolidation test would mean that an increase in vertical pressure would induce a greater increase in horizontal pressure. For SB1, the Cam Clay model does not predict a reasonable lateral stress for a condition of zero lateral strain. The Cam Clay model prediction is not included in Figure 4.15 since it is not reasonable.

The comparison of the cam clay models with the isotropic consolidation test IC_1 is shown in Figure 4.16. The comparison is good since the isotropic normal compression and rebound relationships were estimated from test IC_1. Both models assume the same compressibility relationships and predict the same isotropic consolidation curve.

Cam Clay and Modified Cam Clay Model Summary

The Cam Clay Model and the Modified Cam Clay Model can be used to predict both drained and undrained behavior with one set of parameter values. The parameter values can be found from a reasonable number of conventional tests. The actual shape of the yield surface for SB1 is a different shape than the yield surfaces used in the Cam Clay and

Modified Cam Clay models. The Cam Clay model gives a better fit to the CU and CD tests of SB1 than the Modified Cam Clay model. The Cam Clay model gives a good fit with the CD test data but over predicts the undrained strength of SB1 in the CU tests. The Cam Clay model predicts a physically unreasonable stress state for K_o consolidation conditions. The Modified Cam Clay model gives a fair prediction of the CD tests and greatly over predicts the undrained shear strength of SB1 for CU tests. The Modified Cam Clay model gives a good prediction of 1-D consolidation tests and predicts a reasonable value for K_o.

4.5 Evaluation of R Model for Soil-Bentonite

The model referred to here as the R model is a simplified version of a more complicated model developed by Kutter and Sathialingam (1992). The Kutter and Sathialingam model is a Modified Cam Clay type model using viscoplasticity to incorporate rate-dependent behavior of clays. The yield surface from this model and the parameter R was incorporated in the R model without the viscoplastic aspects. The yield surface is comprised of two different ellipses that can be controlled with the parameter R. The hardening parameter, p'_o, is the same as the hardening parameter in the Modified Cam Clay model. The yield function for the two ellipses, as formulated by Kutter and Sathialingam (1992), are:

ellipse 1:
$$f = (p' - p'_o)\left[p' + \left(\frac{R-2}{R}\right)p'_o\right] + (R-1)^2\left(\frac{q}{M}\right)^2 = 0 \qquad (4.31)$$

ellipse 2:
$$f = p'\left(p' - 2\frac{p'_o}{R}\right) + \left(\frac{q}{M}\right)^2 = 0 \qquad (4.32)$$

where

$$R = \frac{p'_o}{p'_x} \qquad (4.33)$$

and p'_x = the intersection of the ellipses with the critical state line. The yield surface (for R=3 and M=1.3) is shown in Figure 4.17 along with other aspects of the model. Like the cam clay models, an associative flow rule is assumed and the plastic potential function, g, is equal to the yield function. When R is equal to 2 in equations 4.31 and 4.32 that define the yield function, the R model is the same as the Modified Cam Clay model. The Cam Clay model assumes a different yield function than that defined by equations 4.31 and 4.32.

Evaluation of R Parameter for SB1

Wroth and Houlsby (1985) refer to a term called the "spacing ratio," r, which is equivalent to the R parameter used by Kutter and Sathialingam (1992). They state that there is limited data available on the values of R for soils. They also state that the range is small for clays and that a reasonable average value for R is 2. The Modified Cam Clay model assumes in its formulation that R=2. The Cam Clay model assumes in its formulation that R=2.72. Both Wroth and Houlsby (1985) and Dafalias and Herrman (1986) agree that R should be regarded as a material property.

Dafalias and Herrman (1986) state that R for a given soil can be determined either graphically from the compressibility relationships or theoretically from the undrained stress path. The R parameter was estimated graphically for SB1 using the compressibility relationships. As shown in Figure 4.18, if the locations of the isotropic consolidation line (icl) and the critical state line (csl) are known, R can be found from the intersection of these lines with the unload-reload line (url). The isotropic consolidation test IC_1 and the CU tests were used to locate the isotropic consolidation line and determine the slope of the line. Test IC_1 was used to determine the slope of the unload-reload line. The CU tests were used to locate the critical state line. According to the graphical method, R has a value of 3.2 for SB1.

The R parameter was also estimated by changing R to fit the shape of the actual yield surface. Four trial values of R (2.5, 3.0, 3.5, and 4.0) were used to fit the estimated shape of the yield surface. As discussed previously, in order to model the effects of aging, an initial value of p'_o greater than the actual consolidation pressure was used. For each value of R, the initial value of p'_o was varied in order to get the best least squared fit with the normalized yield points. Six points were used to represent the yield point data from Figure 4.8. The most overconsolidated points on the M line were not used in the regression. The three points clustered together were treated as one point in the regression since they were for tests performed under identical conditions. The shape of the yield surfaces for the four values of R are shown in Figure 4.19. Of the four yield surfaces, the value of R=3.5 gives the best least squares fit. All four values of R were used to evaluate the model's ability to represent the behavior of SB1.

Comparison of R Model with Laboratory Tests on SB1

Spreadsheet programs were developed to model triaxial CU and CD tests with the R model. The comparison of the R model with different R values and the representative CU test for SB1 is shown in Figure 4.20. The representative curve is shown by the solid line with the open circles. A different initial p'_o value was used with each R value, as indicated in Figure 4.19. It can be seen from Figure 4.20 that the shape of the undrained stress path is controlled by the R parameter. The curve with R=4.0 is the closest to the representative curve. It gives a very good fit for the stress path, the stress-strain curve, and pore pressure curve. Kutter and Sathialingam (1992) state that a value of R that is close to "optimal" can be obtained by curve fitting the undrained stress path of a normally consolidated CU test. As the values of R decrease, the stress path becomes less flat and the undrained strength increases. At a value of R=2, the R model is the same as the Modified Cam Clay model.

The comparison of the R model with the representative CD test is shown in Figure 4.21. The representative curve is shown with the plain solid line. All of the R models predict the same stress path and the same strength. The strength is a function of the initial stress state and the M value, which is the same for all of the R models. The R models all over predict the axial strain in the stress-strain plot. The R=2.5 curve is fairly close to the representative plot and the R=4 curve grossly over predicts the axial strain. All of the R models underpredict the volumetric strain. The R=2.5 curve is the closest to the representative plot. The results for the CD tests are the opposite of the CU test results, for which R=4 provided the best fit and R=2.5 provided the worst fit.

Application of the R model to one-dimensional consolidation is the same as the Modified Cam Clay model, as previously shown in Figure 4.15. All of the cam clay type models assume the same compressibility relationships and predict the same relationship of volumetric strain versus vertical effective stress for K_o consolidation. However, the models do predict different K_o and η_{Ko} values. This means that the models predict different relationships between volumetric strain and mean effective stress for 1-D compression.

Kutter and Sathialingam (1992) used the relationship between volumetric strain and shear strain for 1-D consolidation in equation 4.29 to solve for η_{Ko} as a function of R. They present the following two equations (Kutter and Sathialingam 1992):

$$\eta_{Ko} = \frac{-3(R-1)^2 + \sqrt{9(R-1)^2 + 4\Delta M^2}}{2\Delta} \tag{4.34}$$

where

$$\Delta = 1 - \frac{9R(R-1)^2(R-2)}{4M^2} \tag{4.35}$$

Using equations 4.28, 4.34 and 4.35, the relationship between K_o and various R values for SB1 are shown in Table 4.3. As R increases, the value of K_o increases. It can be seen in

the table that the value of K_o is in reasonable agreement with the experimentally determined value of K_o=0.57 for R=2, but that an unreasonably high value of K_o is generated when R=4.

Table 4.3 Values of K_o for R Model with M=1.3

R Value	K_o Value
2.0	0.63
2.5	0.76
3.0	0.84
3.5	0.88
4.0	0.91
4.5	0.93

The R model predicts the same isotropic consolidation response as the cam clay models, which was previously presented.

R Model Summary

The R model is a Modified Cam Clay type model with a yield surface that can be varied with the R parameter. Using R values greater than the values assumed in the Modified Cam Clay model (R=2.0) and the Cam Clay model (R=2.7), provides a yield surface that is closer to the observed yield surface for SB1. A value of R=3.5 gives a good fit with the yield surface for SB1. Increasing the value of R to 4 enables a good prediction of the undrained shear strength and good overall fit of the CU test. However, this R value produces large over predictions of the axial strain in the CD tests. If a smaller value of R is used (R=2.5), a good prediction of the CD tests is possible, but the model is a bad fit of the CU tests; the undrained shear strength is greatly over predicted. The model gives a good prediction of 1-D consolidation. The predicted value of K_o is dependent on the R value.

4.6 Evaluation of RS Model for Soil-Bentonite

The model referred to here as the R model is a simplified version of the more complicated model developed by Kutter and Sathialingam (1992) described in the previous section. The RS model incorporates the yield surface from the model by Kutter and Sathialingam (1992) and assumes a non-associative flow rule. The model by Kutter and Sathialingam is formulated assuming an associative flow rule, although the authors mention the possibility of a non-associative flow rule. The RS model has a yield function that can be varied with the parameter R, and a plastic potential function that can be varied with a parameter referred to here as the S parameter. The yield surface and the plastic potential function are each described by the functions of the same form as used in the model by Kutter and Sathialingam (1992). The functions are made up of two ellipses as shown in Figure 4.22. The size parameter for the yield function is the p'_o parameter. The size parameter for the plastic potential function is referred to here as the p'_{og} parameter.

The yield surface is comprised of two ellipses as formulated by Kutter and Sathialingam (1992):

ellipse 1:
$$f = (p' - p'_o)\left[p' + \left(\frac{R-2}{R}\right)p'_o\right] + (R-1)^2\left(\frac{q}{M}\right)^2 = 0 \tag{4.31}$$

ellipse 2:
$$f = p'\left(p' - 2\frac{p'_o}{R}\right) + \left(\frac{q}{M}\right)^2 = 0 \tag{4.32}$$

where

$$R = \frac{p'_o}{p'_x} \tag{4.33}$$

Similarly, the plastic potential function is comprised of two ellipses as given by:

ellipse 1:
$$g = (p' - p'_{og})\left[p' + \left(\frac{S-2}{S}\right)p'_{og}\right] + (S-1)^2\left(\frac{q}{M}\right)^2 = 0 \tag{4.36}$$

ellipse 2: $$g = p'\left(p' - 2\frac{p'_{og}}{S} \right) + \left(\frac{q}{M} \right)^2 = 0 \qquad (4.37)$$

where

$$S = \frac{p'_{og}}{p'_{xg}} \qquad (4.38)$$

and p'_{xg}= the intersection of the plastic potential function with the critical state line. The yield surface (with R=3) and plastic potential surface (with S=3.5) for M=1.3 are shown in Figure 4.22.

The RS model becomes the R model when R is equal to S. The RS model becomes the Modified Cam Clay model when R and S are both equal to 2.

Shape of the Actual Plastic Potential Function

The shape of the plastic potential function determines the relative magnitudes of the incremental plastic shear strain and the incremental plastic volumetric strain. The outward normal vector to the plastic potential function is called the plastic strain increment vector, which gives the relative magnitudes of the plastic strains, as shown in Figure 4.22. The actual magnitude of plastic volumetric strain is determined from the compressibility relationships, the shape of the yield function, and the stress increments.

The CD tests on SB1 were used to determine the shape of the actual plastic potential function. The change in the length of the sample $\delta\ell$ and the change in the volume of the sample δV were measured during the CD test. The axial and volumetric strain were calculated from the following respective equations:

$$\delta\varepsilon_{axial} = \frac{-\delta\ell}{\ell} \qquad (4.39)$$

$$\delta\varepsilon_p = \frac{-\delta V}{V} \tag{4.40}$$

For a triaxial specimen, assuming right circular cylinder deformation, the following relationship among shear strain, axial strain, and volumetric strain (Wood 1990) holds:

$$\delta\varepsilon_q = \delta\varepsilon_{axial} - \frac{1}{3}\delta\varepsilon_p \tag{4.41}$$

The elastic portion of the strains were estimated using the elastic parameters and the following equations (from equations 4.11, 4.13, and 4.22):

$$\delta\varepsilon_p^e = \frac{\kappa\delta p'}{vp'} \tag{4.11}$$

$$\delta\varepsilon_q^e = \frac{2(1+\nu')\kappa}{9(1-2\nu')vp'}\delta q \tag{4.42}$$

The incremental plastic strains were estimated by subtracting the elastic strains from the total strains as follows using equations 4.11, 4.41, and 4.42:

$$\delta\varepsilon_p^p = \delta\varepsilon_p - \frac{\kappa\delta p'}{vp'} \tag{4.43}$$

$$\delta\varepsilon_q^p = \delta\varepsilon_{axial} - \frac{1}{3}\delta\varepsilon_p - \frac{2(1+\nu')\kappa}{9(1-2\nu')vp'}\delta q \tag{4.44}$$

For each CD test, at a point just after the yield point (away from the transition), a small incremental value of stress (δp, δq) was analyzed to evaluate equations 4.43 and 4.44. For the stress increment, the axial and volumetric strain increment was estimated from the plots shown in Section 3.5. The plastic volumetric strain and plastic shear strains were evaluated from equations 4.43 and 4.44; and the direction of the plastic strain increment vector was calculated. The direction of the plastic strain increment vector was also estimated for the isotropic consolidation test IC_2.

The results are shown in Figure 4.23. In the figure, the plastic strain increment vectors of a convenient length are plotted at each of the yield points, although the plastic strain increment vector was evaluated over a stress increment just after the yield point. The plastic potential function should be perpendicular to the plastic strain increment vector. It can be seen that no smooth curve could be drawn perpendicular through all of the points. However, a different curve satisfying perpendicularity could be drawn through each yield point. The data suggest that these curves would have different sizes but have the same general shape. In order to estimate the shape of one plastic potential function, the plastic strain increment vectors were projected along lines of constant η until a smooth curve could be drawn perpendicular to the vectors. The estimated shape of the plastic potential function is shown in Figure 4.24 with the dashed line. The plastic strain increment vectors are plotted at the yield points (open circles). The projected plastic stain increment vectors are shown as solid lines plotted at points that are estimated to be on the plastic potential function. Points on the plastic potential function are shown as black circles. At a η value greater than M, no information is available on the shape of the yield surface.

Evaluation of S Parameter for SB1

The S parameter describes the shape of an elliptical plastic potential function for the RS model. The shape of the estimated plastic potential function for SB1 (in Figure 4.24) to the right side of the M line, is very close to an ellipse. A plastic potential function with S=3.1 is shown in Figure 4.25. The points from Figure 4.24, estimated to be on the plastic potential function for SB1, are also shown. A value of S=3.1 gives a very good fit with the data.

Effect of R and S Parameters

Using the RS model, the values of R and S were varied in order to see their effect on stress-strain behavior and to find the optimum pair for SB1. The effect of varying R on modeling the CU test is shown in Figure 4.26. R was varied from 2.5 to 4.0 and S was

kept constant at 3.0. The results are essentially the same as varying R using the R model in Figure 4.20 (where R and S are always the same value). R controls the shape of the undrained stress path and the undrained shear strength, and the value of S has very little effect. The value of R=4.0 gives the best fit with the representative CU curve for SB1.

The effect of varying R on modeling the CD test is shown in Figure 4.27. Again, R was varied from 2.5 to 4.0 and S was kept constant at 3.0. The stress-strain curves are all very similar and varying the R value has little effect. The stress strain curves are similar to the curve in Figure 4.21 corresponding to the R model where R=3.0 and S=3.0. Thus, the shape of the drained stress-strain curve is controlled by the S parameter, and the R parameter has very little effect. Using a value of S=3.0 does not give a good fit with the stress-strain curve of the representative CD test for SB1. Varying the R value has an effect on the volumetric strain prediction. Increasing R increases the predicted volumetric strain.

The effect of varying S on modeling the CU test is shown in Figure 4.28. The S parameter was varied from 2.0 to 3.0 and R was kept constant at 3.0. Varying S has no effect on the undrained stress path and virtually no effect on the stress-strain curve or excess pore pressure plot.

The effect of varying S on modeling the CD test is shown in Figure 4.29. The S value was varied from 2.0 to 3.0 while R was kept constant at 3.0. It can be seen that the S value controls the shape of the stress-strain curve. As S increases, the stress-strain curve becomes less stiff. The value of 2.0 provides a good fit with the stress-strain curve. Varying the S value also affects the volumetric strain plot. Increasing the S value decreases the volumetric strain prediction. Based on the results in Figures 4.27 and 4.29, it appears that increasing the value of R/S has the effect of increasing the volumetric strain.

Comparison of RS Model with Laboratory Tests on SB1

Various combinations of R and S were evaluated in order to find the best fit with the laboratory test data for SB1. The results are consistent with the results of varying R and S separately. A good fit for both CU and CD tests was obtained with R=4.0 and S=2.0. The R value previously estimated from the compressibility relationships was 3.2. The R value estimated from the yield surface was 3.5. The S value estimated from measuring the plastic strains at yield was 3.1. These methods seem to provide a rough estimate but it appears necessary to use both drained and undrained laboratory test data to find the optimal pair. It is also much easier to use a few CU and CD tests than to experimentally determine the yield surface and the plastic potential surface.

The results of using R=4.0 and S=2.0 for modeling the CU test is shown in Figure 4.30. The model gives a very good fit for all of the plots. The results of using R=4.0 and S=2.0 for modeling the CD tests is shown in Figure 4.31. The model gives a very good fit for the stress path and stress-strain curve. The model over predicts the amount of volumetric strain by approximately 17%. The magnitude of the over prediction is approximately 1% volumetric strain of the sample.

The prediction of 1-D consolidation using the RS model is the same as the prediction using the Modified Cam Clay model, shown in Figure 4.15, since it assumes the same compressibility relationships. Using equation 4.29, the same procedure used for the R model can be used to find the relationship between η_{ko} and the model parameters. The relationship is controlled by the plastic potential function whose shape is control by R with the R model and S with the RS model. The relationship between η_{Ko} and S is given by the following:

$$\eta_{Ko} = \frac{-3(S-1)^2 + \sqrt{9(S-1)^2 + 4\Delta M^2}}{2\Delta} \qquad (4.45)$$

where

$$\Delta = 1 - \frac{9S(S-1)^2(S-2)}{4M^2} \tag{4.46}$$

The relationship between K_o and S is shown in Table 4.4. The value of K_o predicted by using S=2.0 is 0.63 which is fairly close to the measured value of K_o=0.57.

Table 4.4 Values of K_o for RS Model with M=1.3

S value	K_o value
2.0	0.63
2.5	0.76
3.0	0.84
3.5	0.88
4.0	0.94
4.5	0.93

The RS model predicts the same isotropic consolidation response as the other cam clay type models, which is a good fit.

Comparison of RS Model with Laboratory Tests on SB3

The RS model was also used to predict laboratory tests on SB3, in order to assess the ability of the model to represent a different soil-bentonite mixture. Representative normalized curves for CU and CD tests performed on SB3 were found. Values for the RS parameters (lambda, kappa, Poisson's ratio, M, and N) for SB3 were found using the same procedures described for SB1. The R and S parameter values were varied in order to find the optimal pair for both CU and CD tests on SB3. The values of R=4 and S=2 were found to provide the best fit for all of the tests. The best R and S parameter values for SB3 are the same as for SB1.

The results of using R=4 and S=2 for modeling the CU test for SB3 is shown in Figure 4.32. The RS model provides a very good fit with the representative CU data for all of

the plots. The results of using R=4 and S=2 for modeling the CD test for SB3 is shown in Figure 4.33. The RS model provides a good fit of the stress-strain curve, but over predicts the volumetric strain, which is similar to results on SB1. The RS model over predicts the volumetric strain by approximately 53%; however, the magnitude of the over prediction is less than 2% volumetric strain of the sample.

The RS parameter values for SB1 and SB3 are summarized in Table 4.5. The compressibility properties are significantly different for the two soil-bentonite mixtures, but the strength values and the R and S values are the same.

Table 4.5 Parameter Values for RS Model for SB1 and SB3

Soil-Bentonite Mixture	λ, lambda	κ, kappa	ν', Poisson's ratio	M	N	R	S
SB1	0.070	0.0048	0.37	1.3	2.044 (p' in psf) 1.696 (p' in psi) 1.834 (p' in kPa)	4	2
SB2	0.039	0.0012	0.48	1.3	1.840 (p' in psf) 1.646 (p' in psi) 1.721 (p' in kPa)	4	2

RS Model Summary

The RS model is a non-associated Modified Cam Clay type model that has parameters to change the yield surface and plastic potential surfaces into ellipses of varying shapes. The R parameter changes the shape of the yield surface, and it has been shown to control the shape of the undrained stress path. The S parameter changes the shape of the plastic potential surface, and it has been shown to control the drained stress-strain response. By varying R and S, an optimum pair was found that provides a good prediction of CU tests, CD tests, and consolidation tests for SB1 and SB3. Of the constitutive models studied, the RS model gives the best representation of soil-bentonite mixtures in conventional laboratory tests.

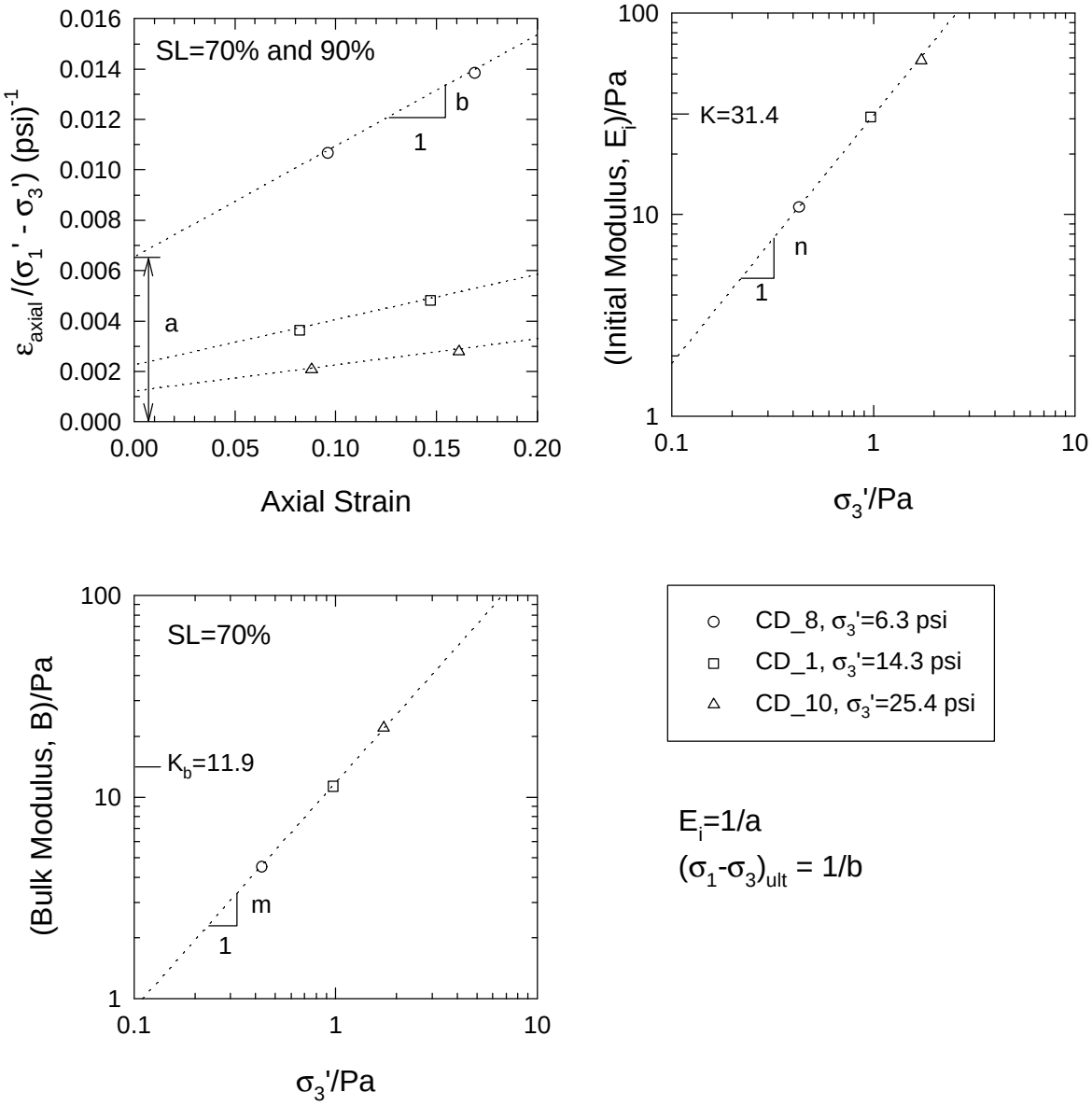

Figure 4.1 Determining Hyperbolic Parameter Values from CD tests on SB1

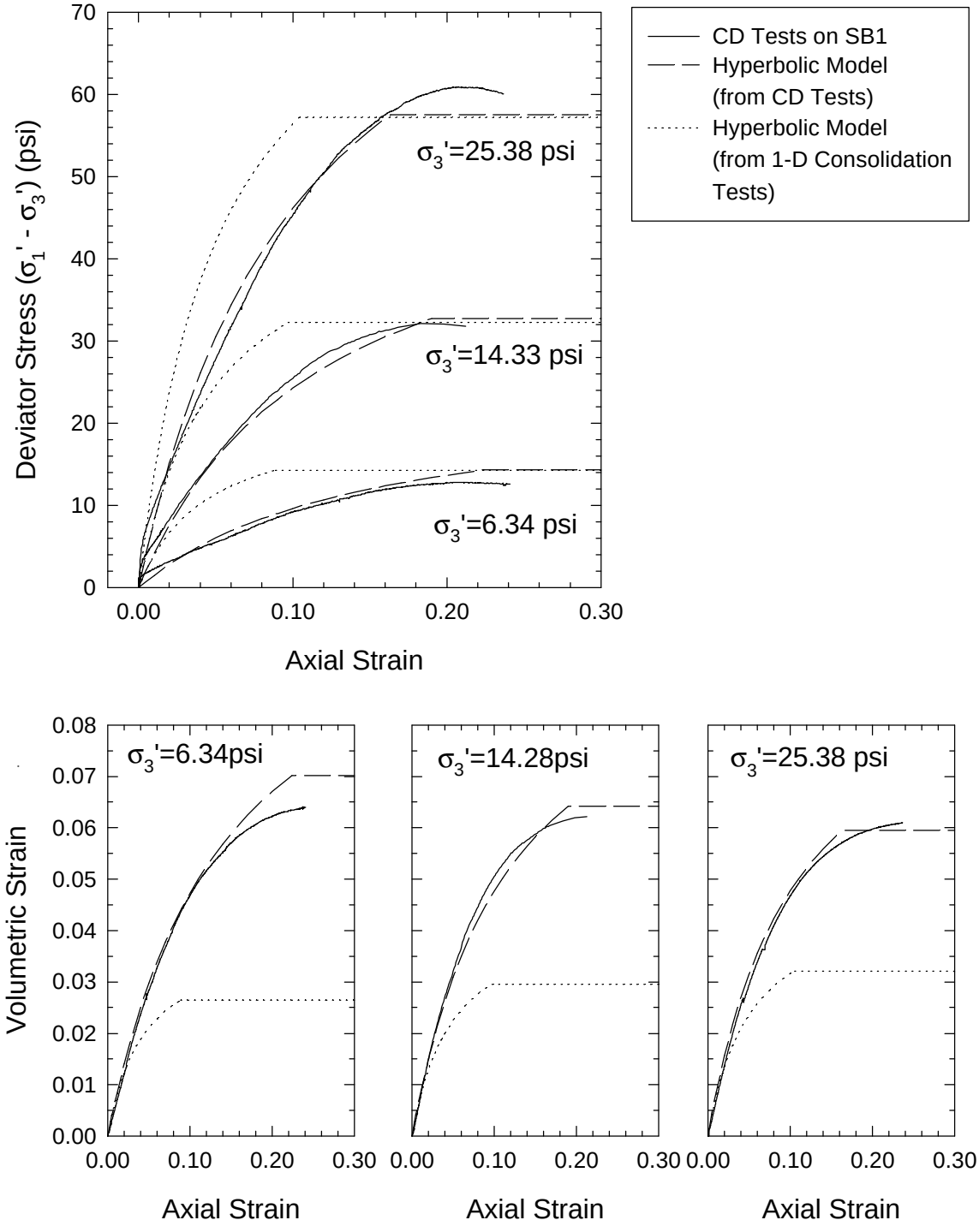

Figure 4.2 Comparison of CD Tests on SB1 and Hyperbolic Model Prediction

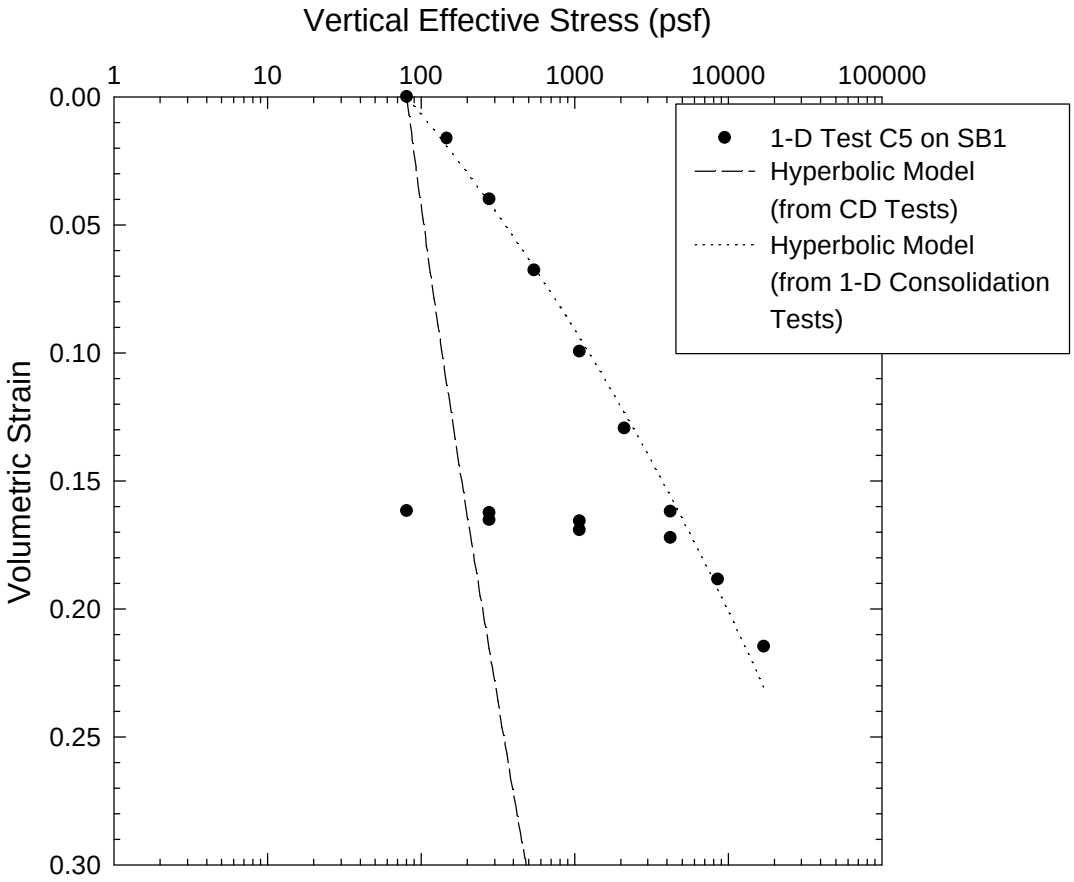

Figure 4.3 Comparison of One-Dimensional Consolidation Test on SB1 and Hyperbolic Model Prediction

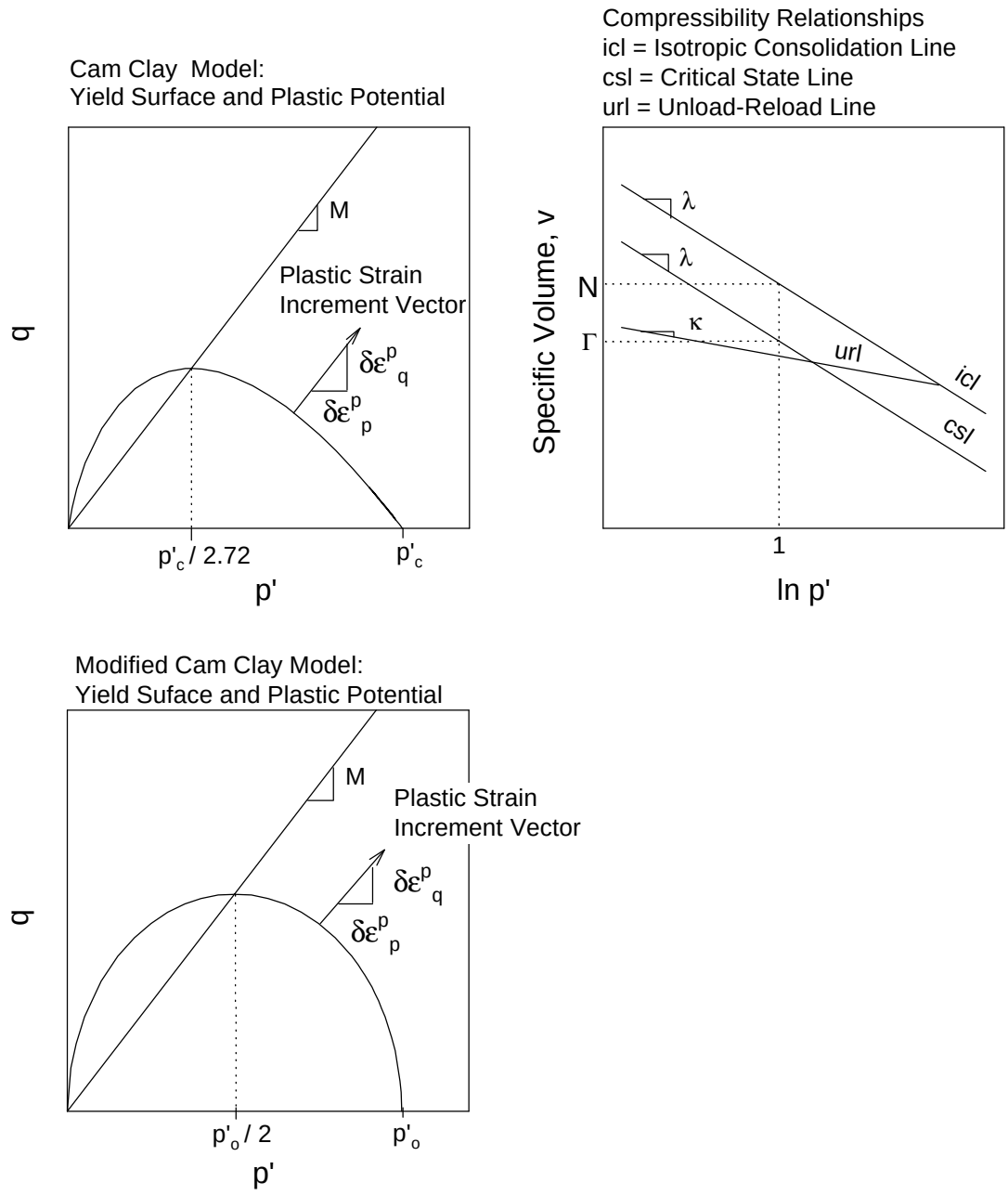

Figure 4.4 Properties of Cam Clay Model and Modified Cam Clay Model

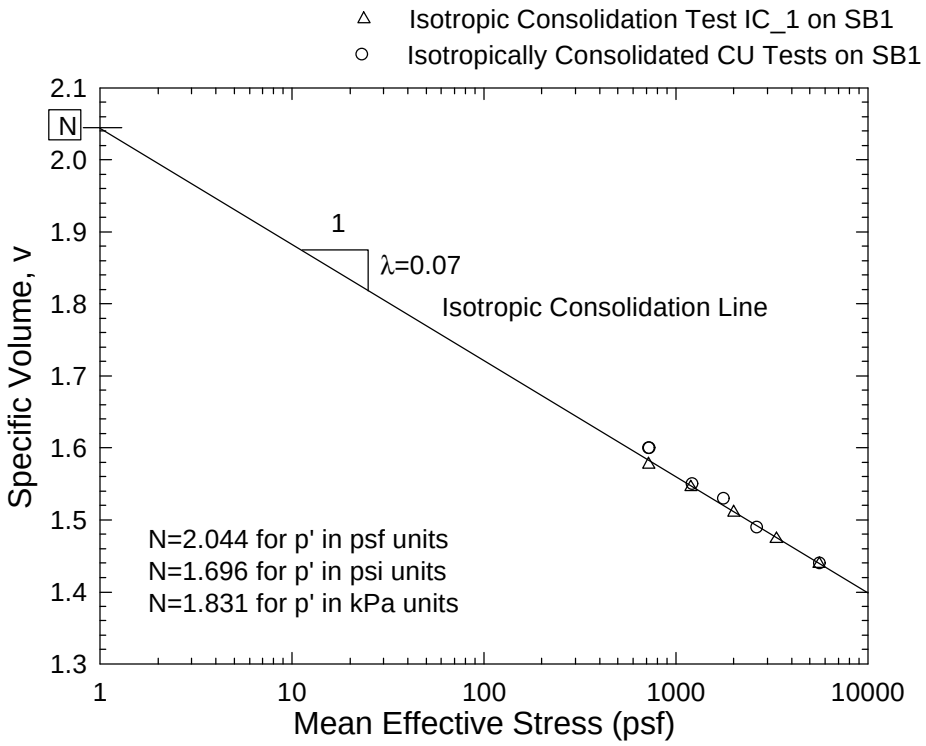

Figure 4.5 Determining N Parameter of Cam Clay Model for SB1

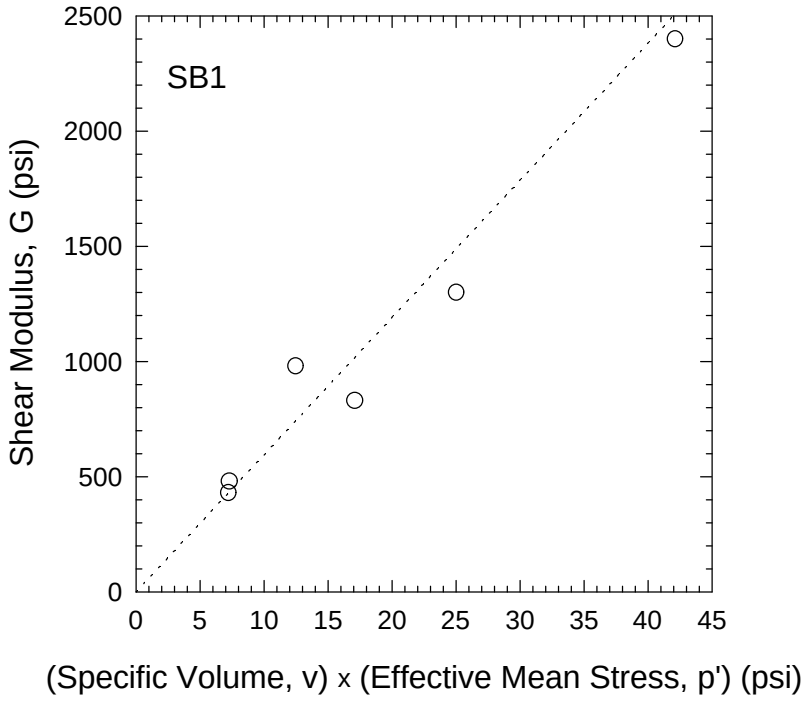

Figure 4.6 Determining Poisson's Ratio for SB1

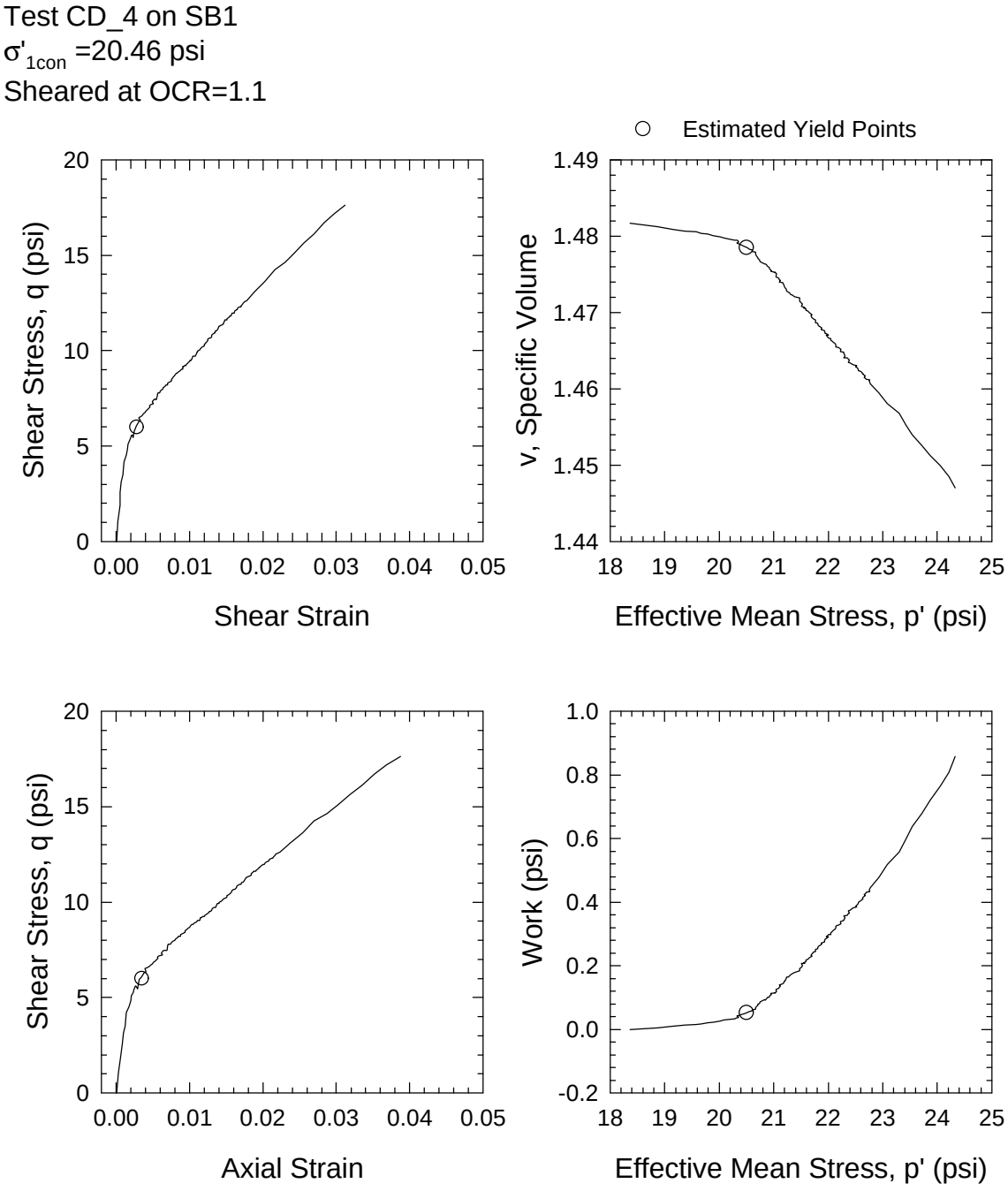

Figure 4.7 Determining the Yield Point for CD_4

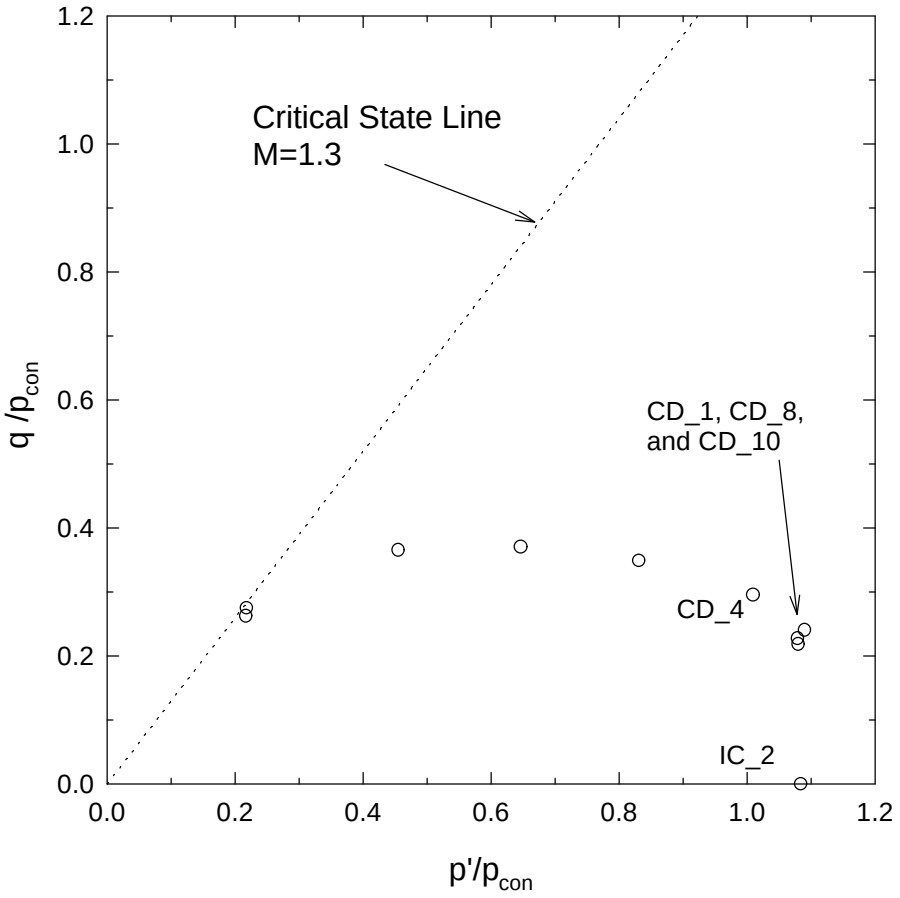

Figure 4.8 Yield Points for SB1 Normalized by the Mean Consolidation Pressure, p_{con}

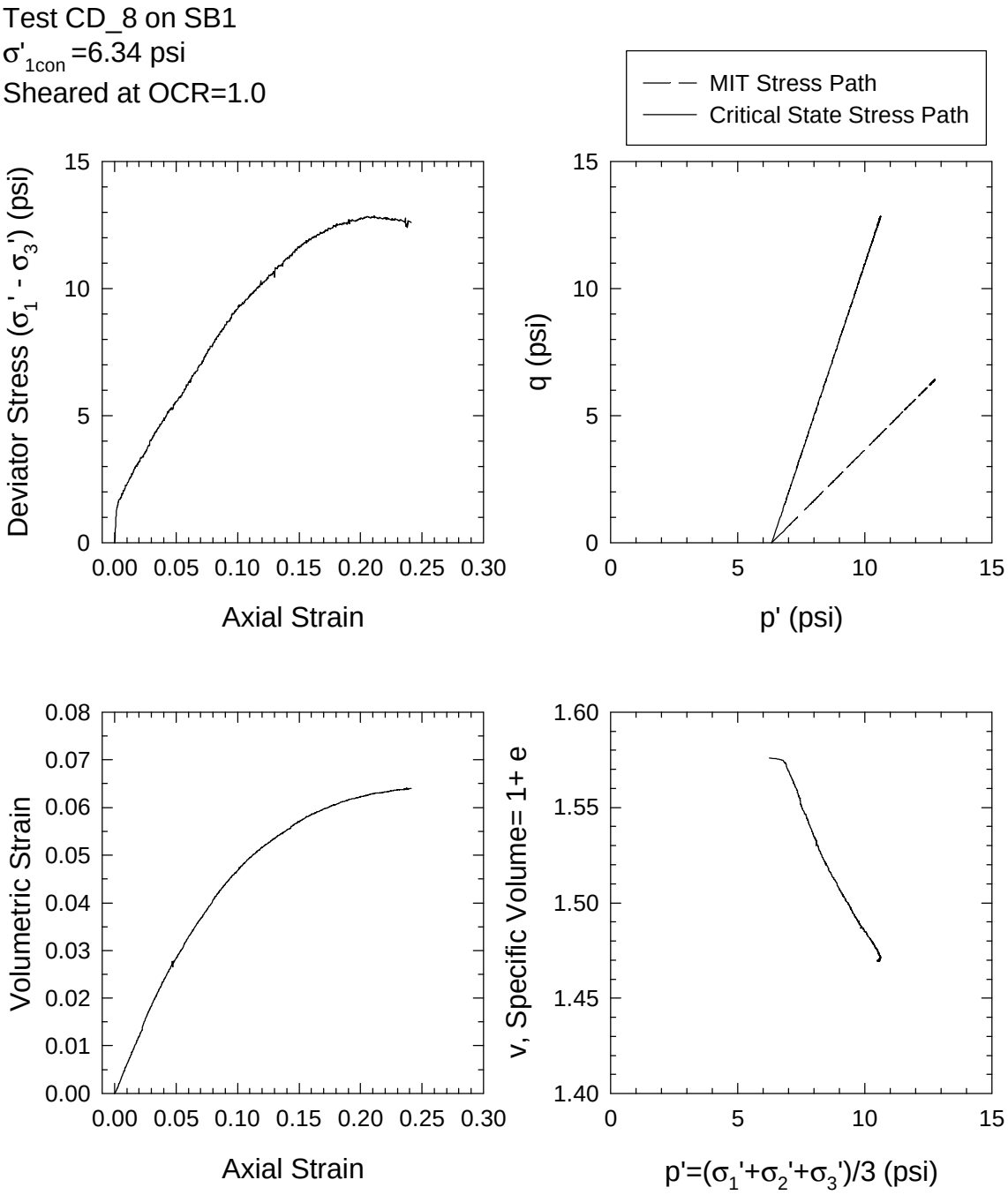

Figure 4.9 Consolidated Drained Triaxial Test CD_8 on SB1

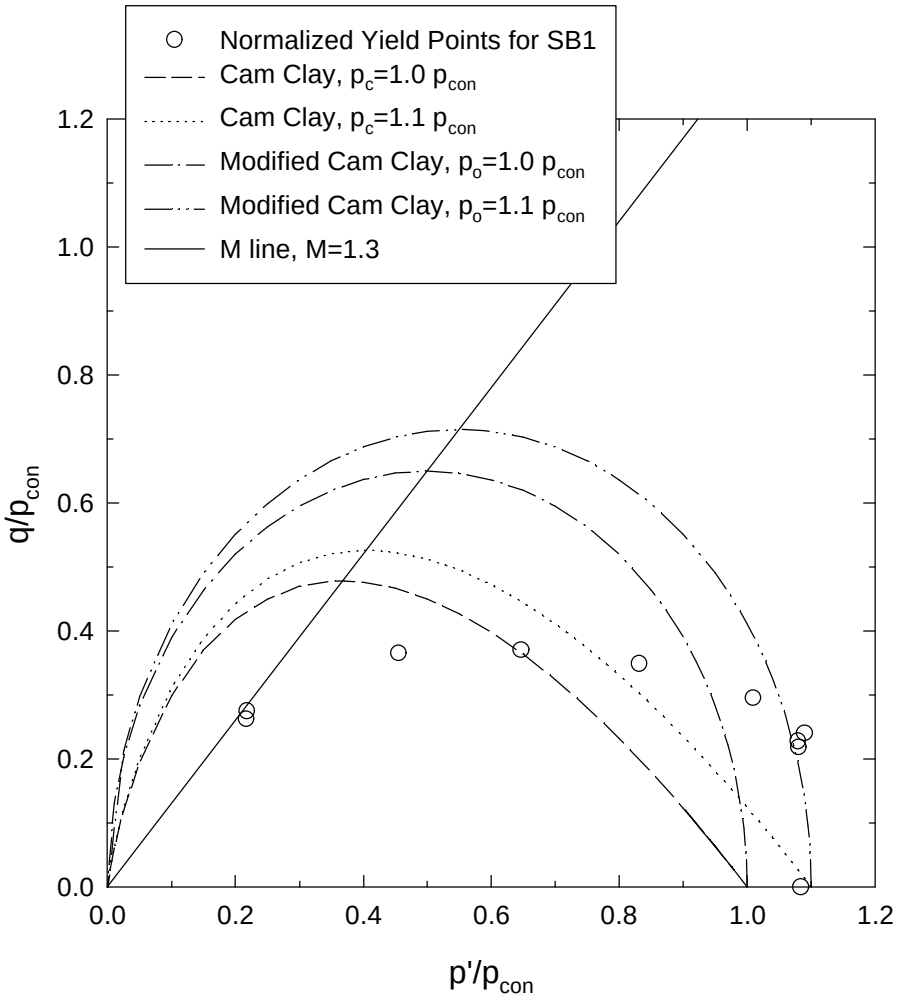

Figure 4.10 Shape of Yield Functions for SB1 and Cam Clay Models

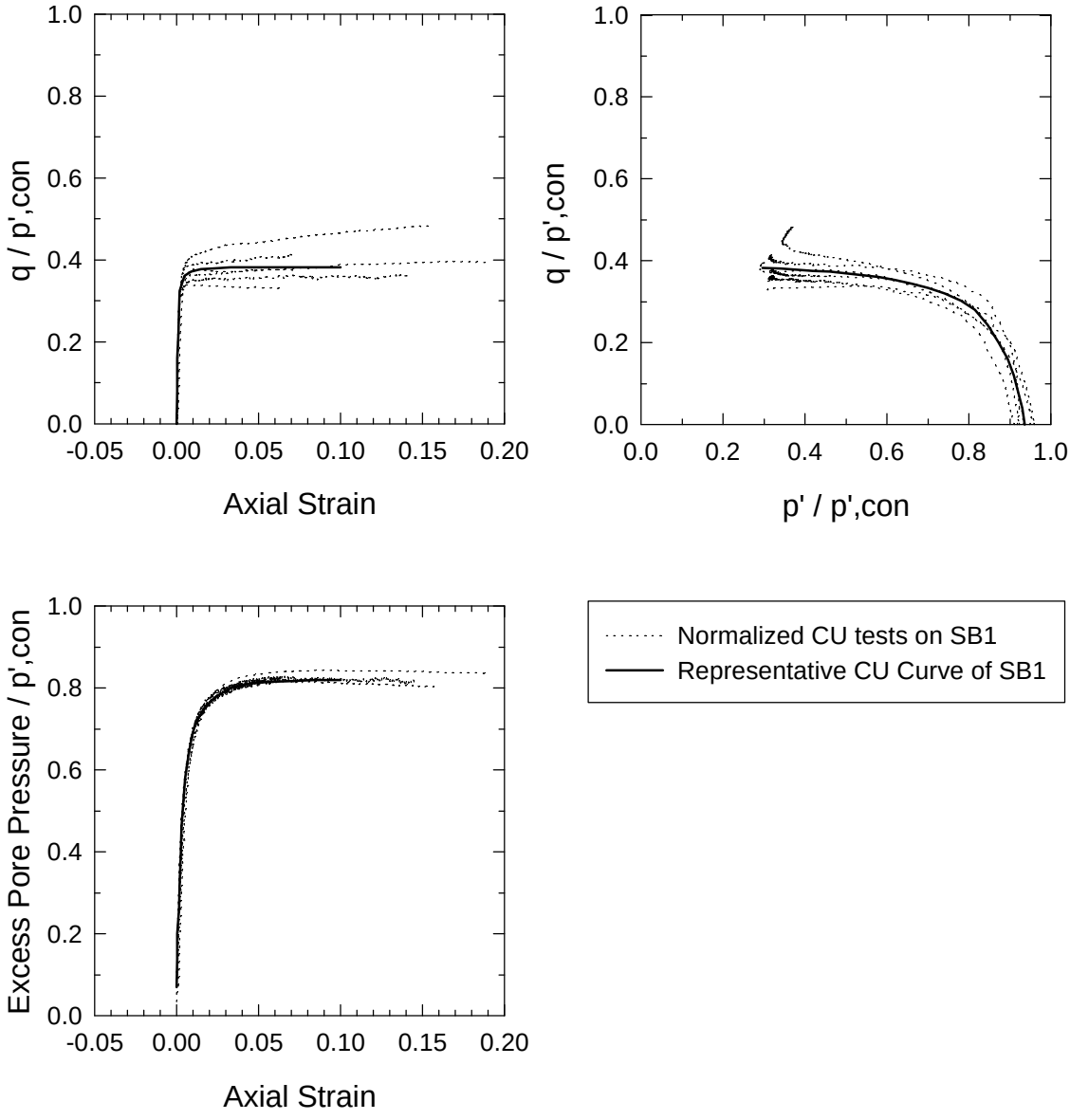

Figure 4.11 Normalized Plots of CU Tests on Normally Consolidated Samples of SB1 with Representative Curves

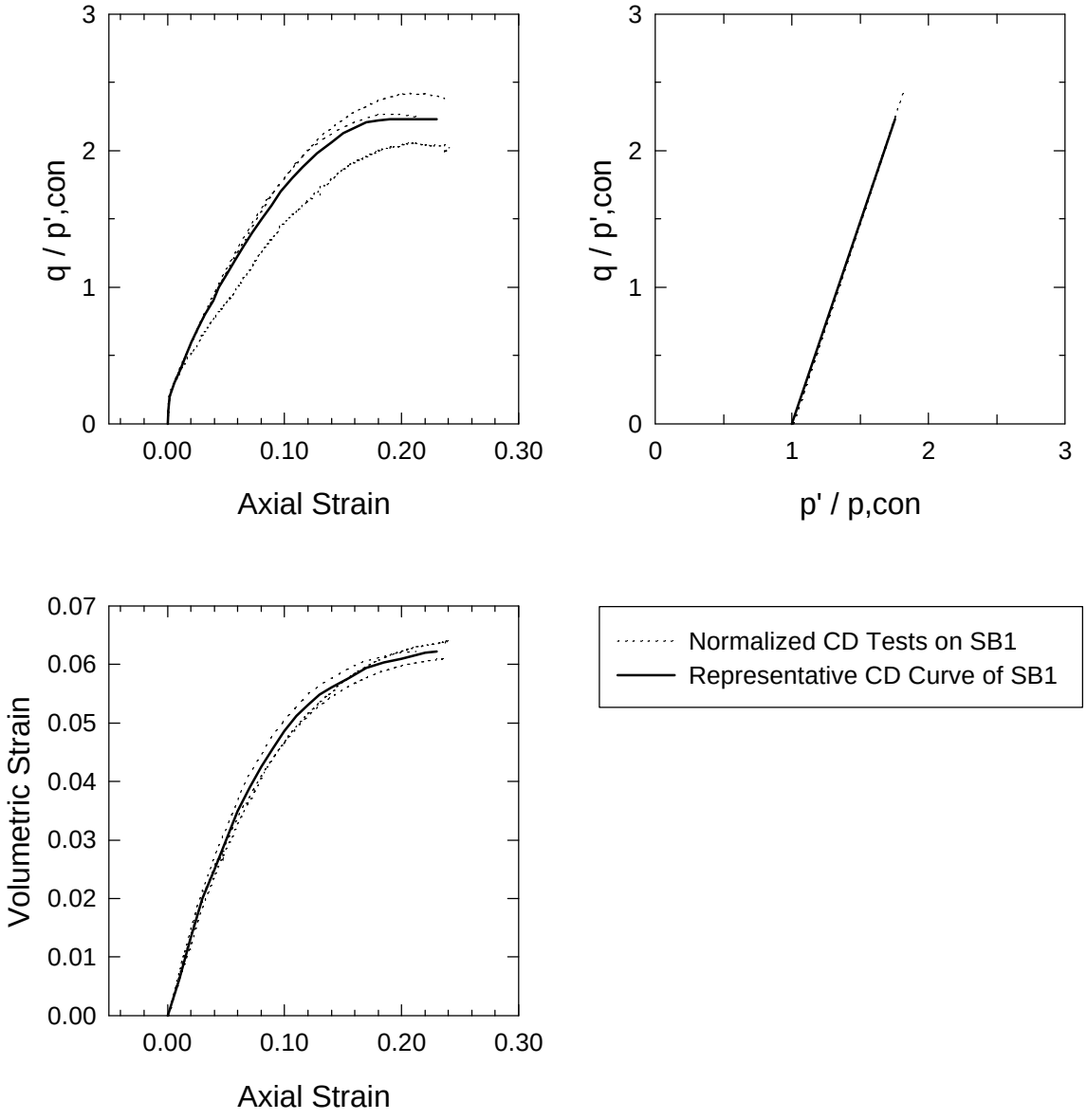

Figure 4.12 Normalized Plots of CD Tests on Normally Consolidated Samples of SB1 with Representative Curves

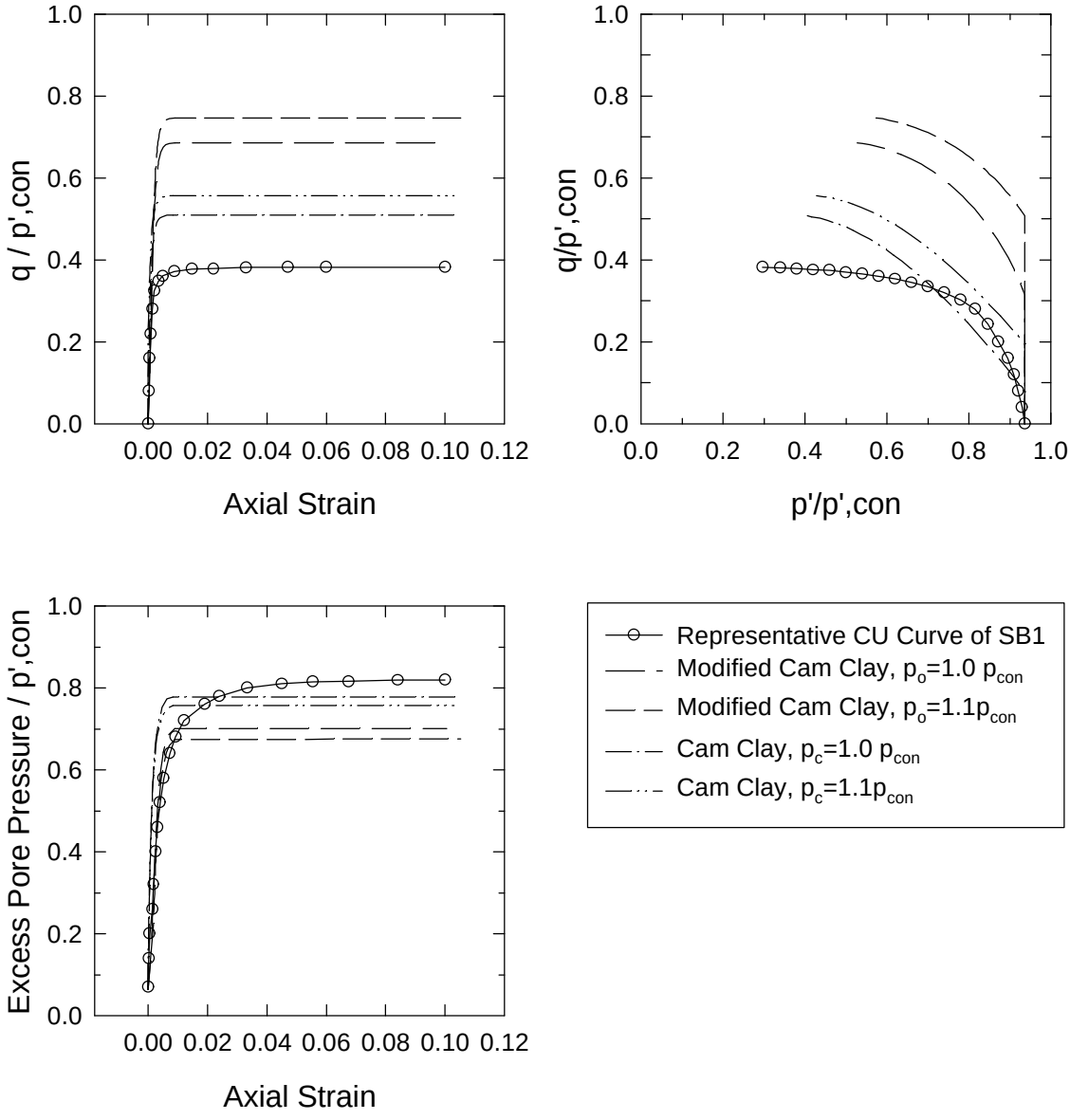

Figure 4.13 Representative Normalized CU Test of SB1 and Cam Clay Models

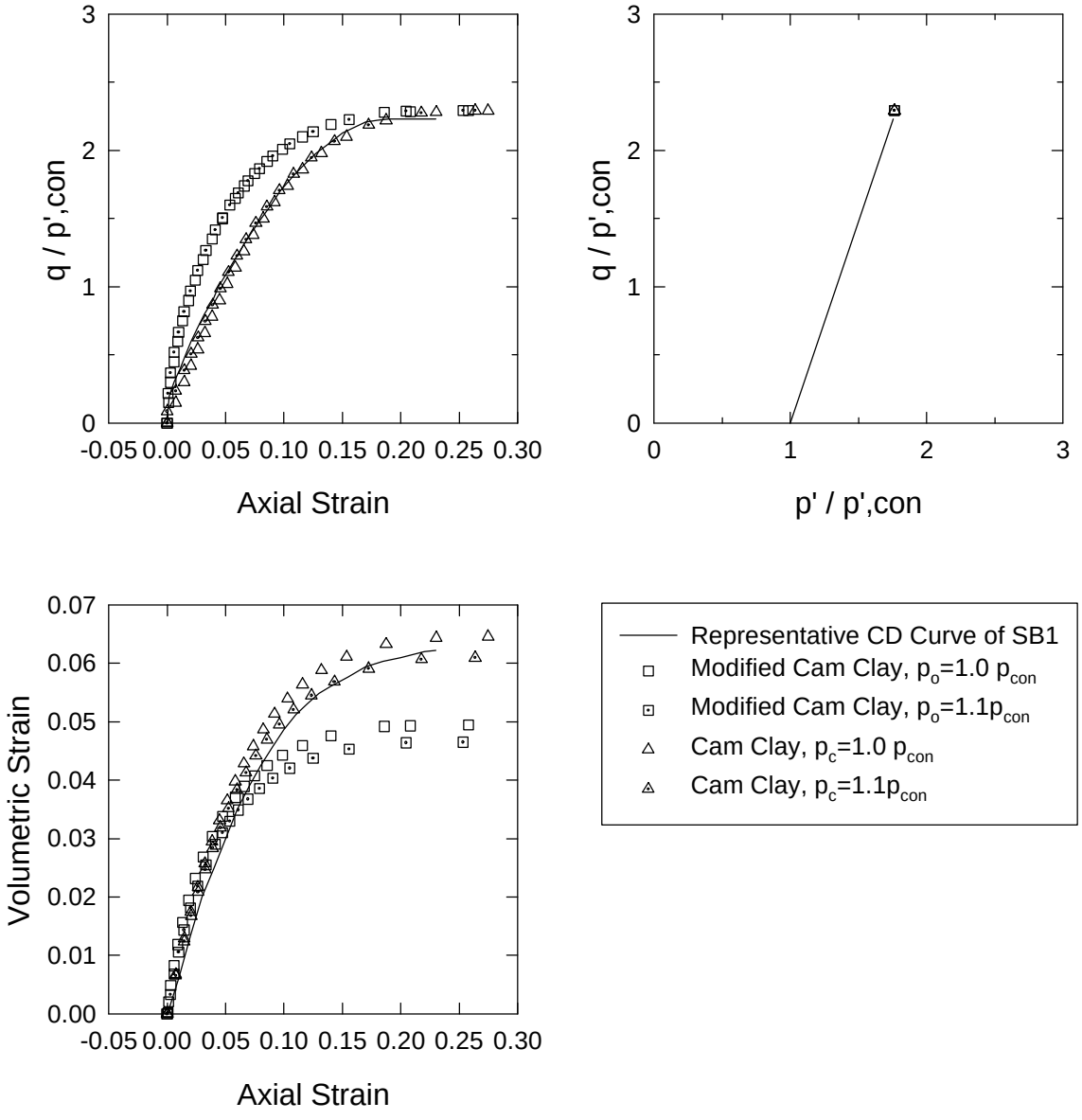

Figure 4.14 Representative Normalized CD Test of SB1 and Cam Clay Models

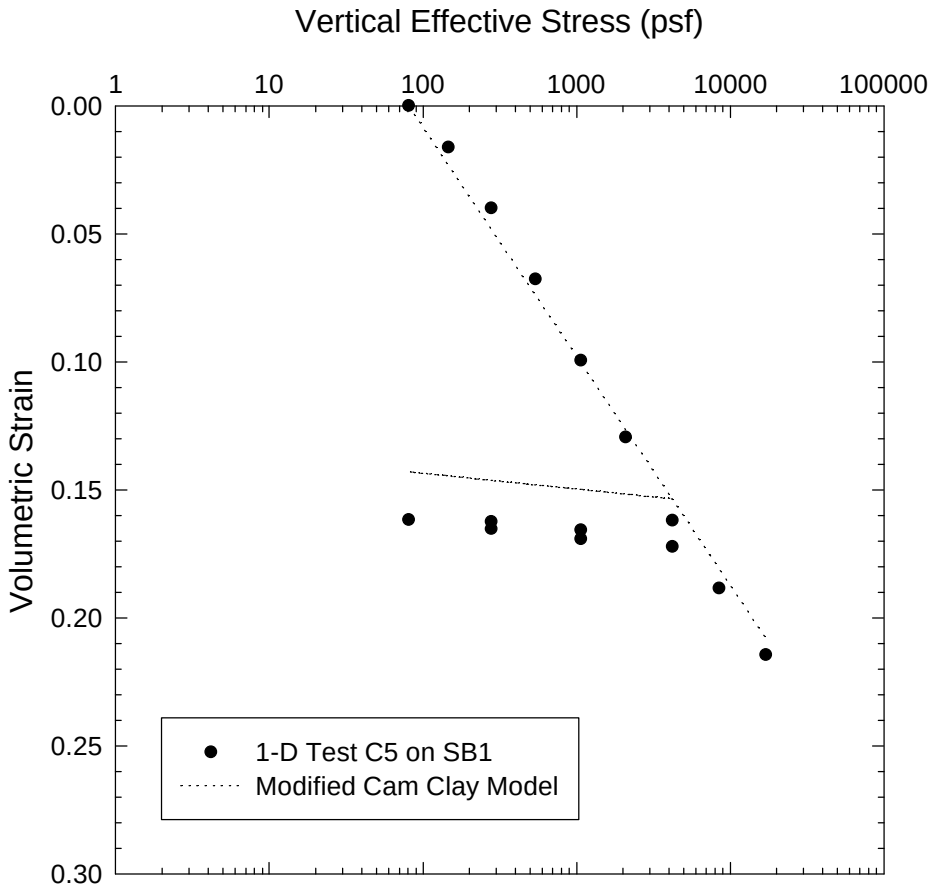

Figure 4.15 Comparison of One-Dimensional Consolidation Test on SB1 with Modified Cam Clay Model

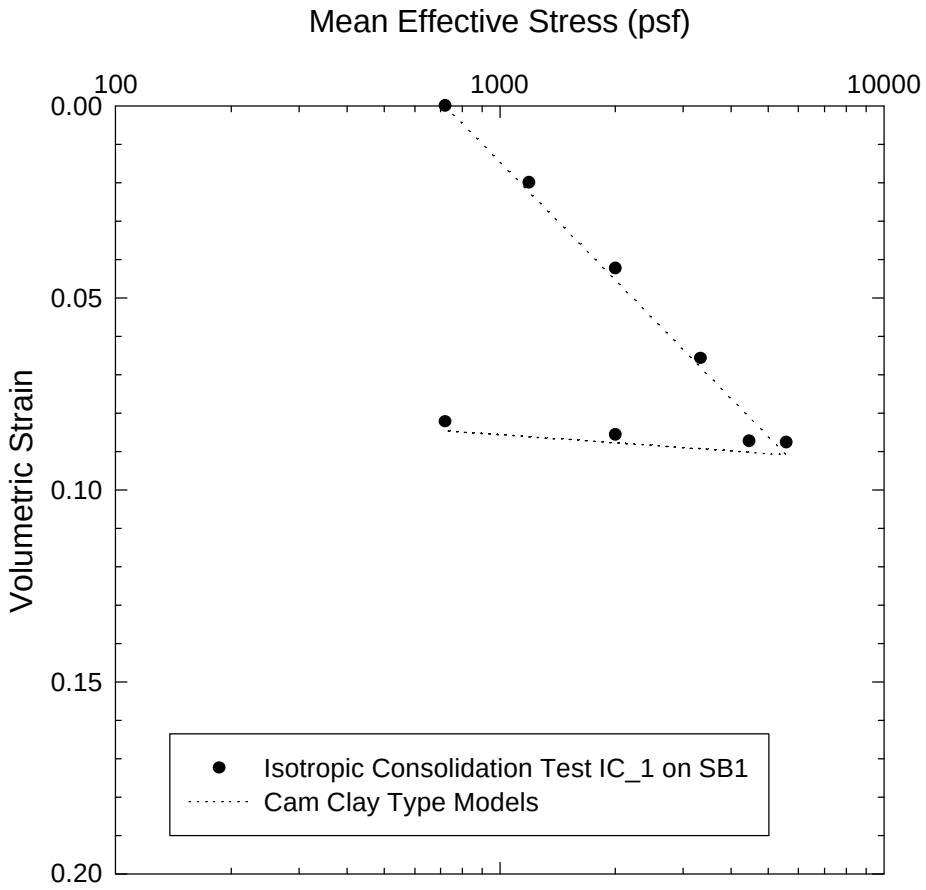

Figure 4.16 Comparison of Isotropic Consolidation Test on SB1 with Cam Clay Type Models

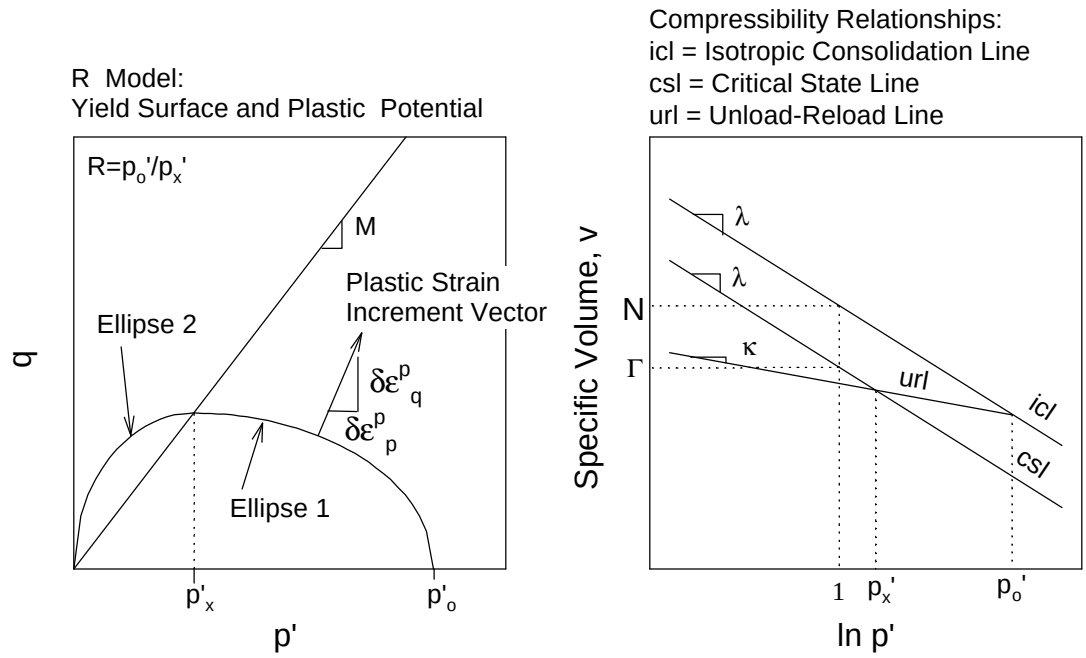

Figure 4.17 Properties of R Model

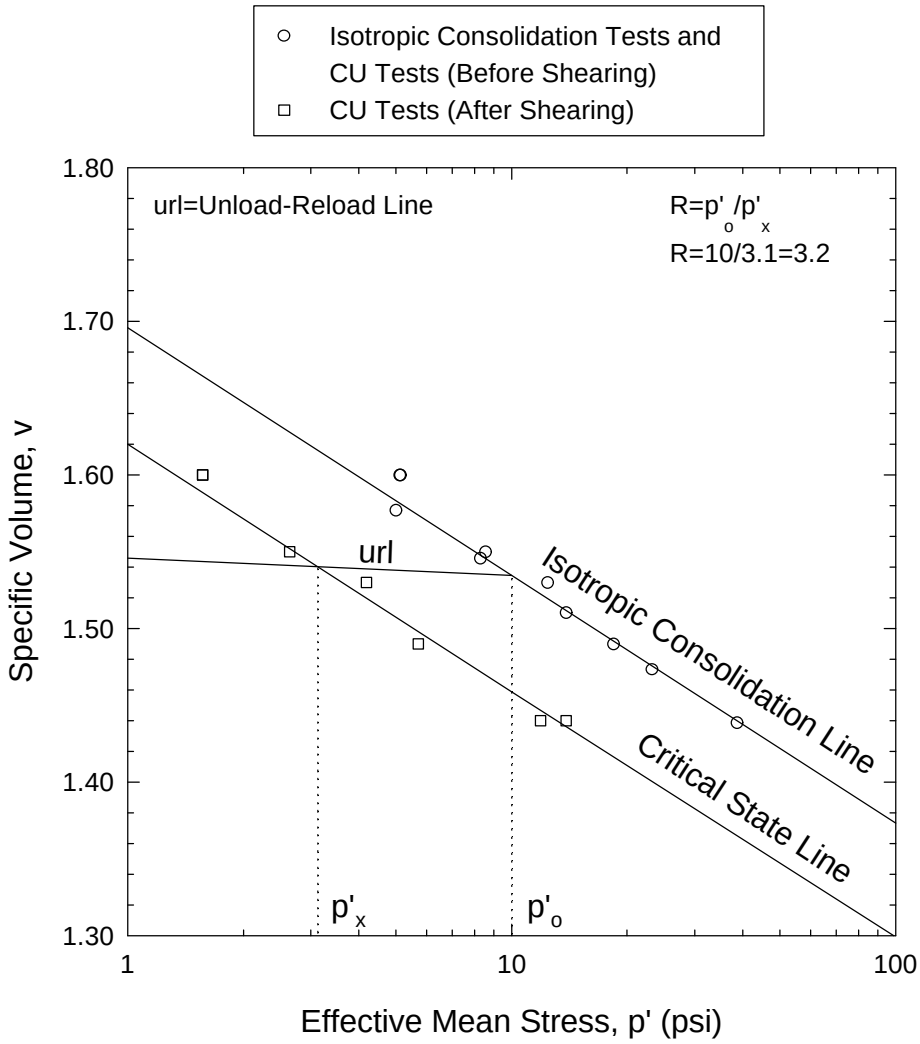

Figure 4.18 Graphical Estimate of R Parameter for SB1

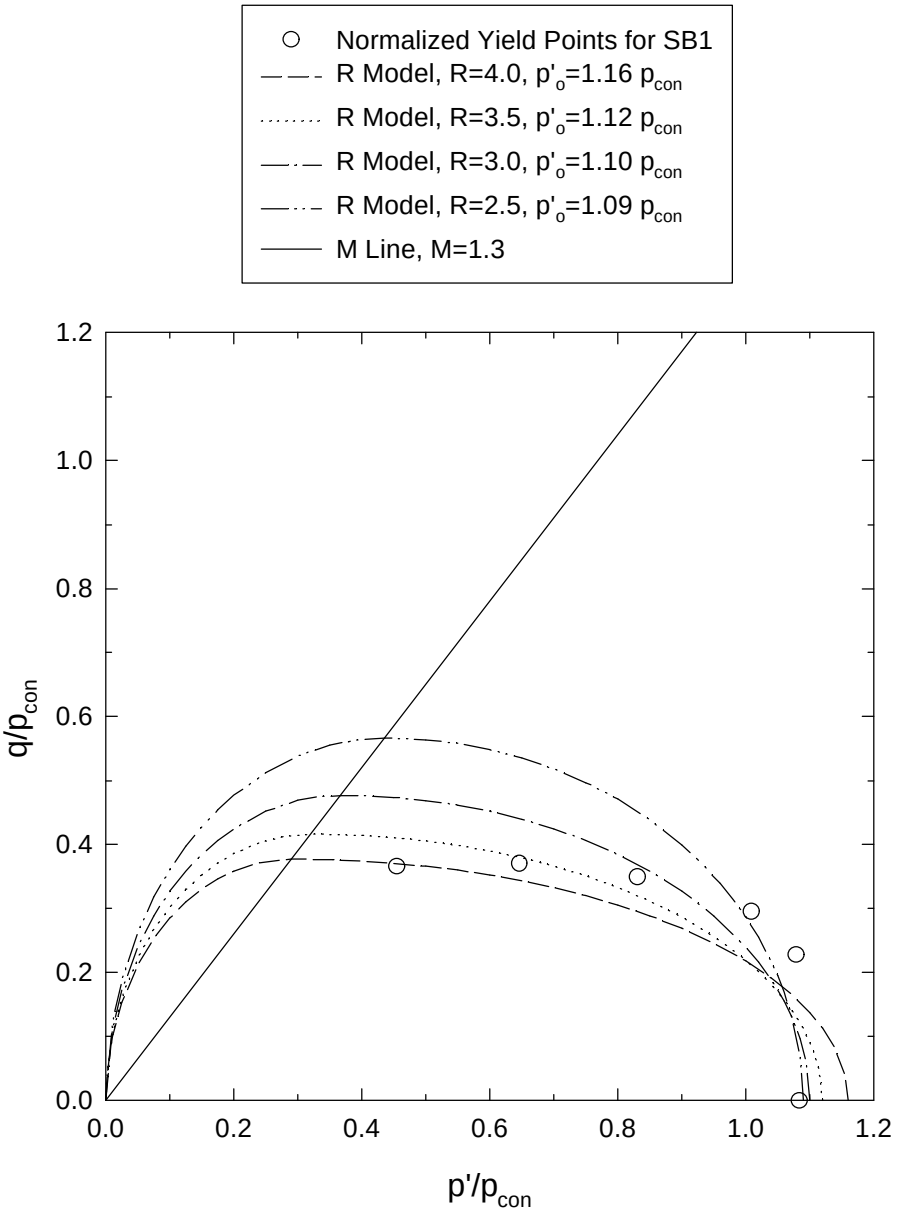

Figure 4.19 Shape of Yield Functions for SB1 and R Model with Various R and p'_o Values

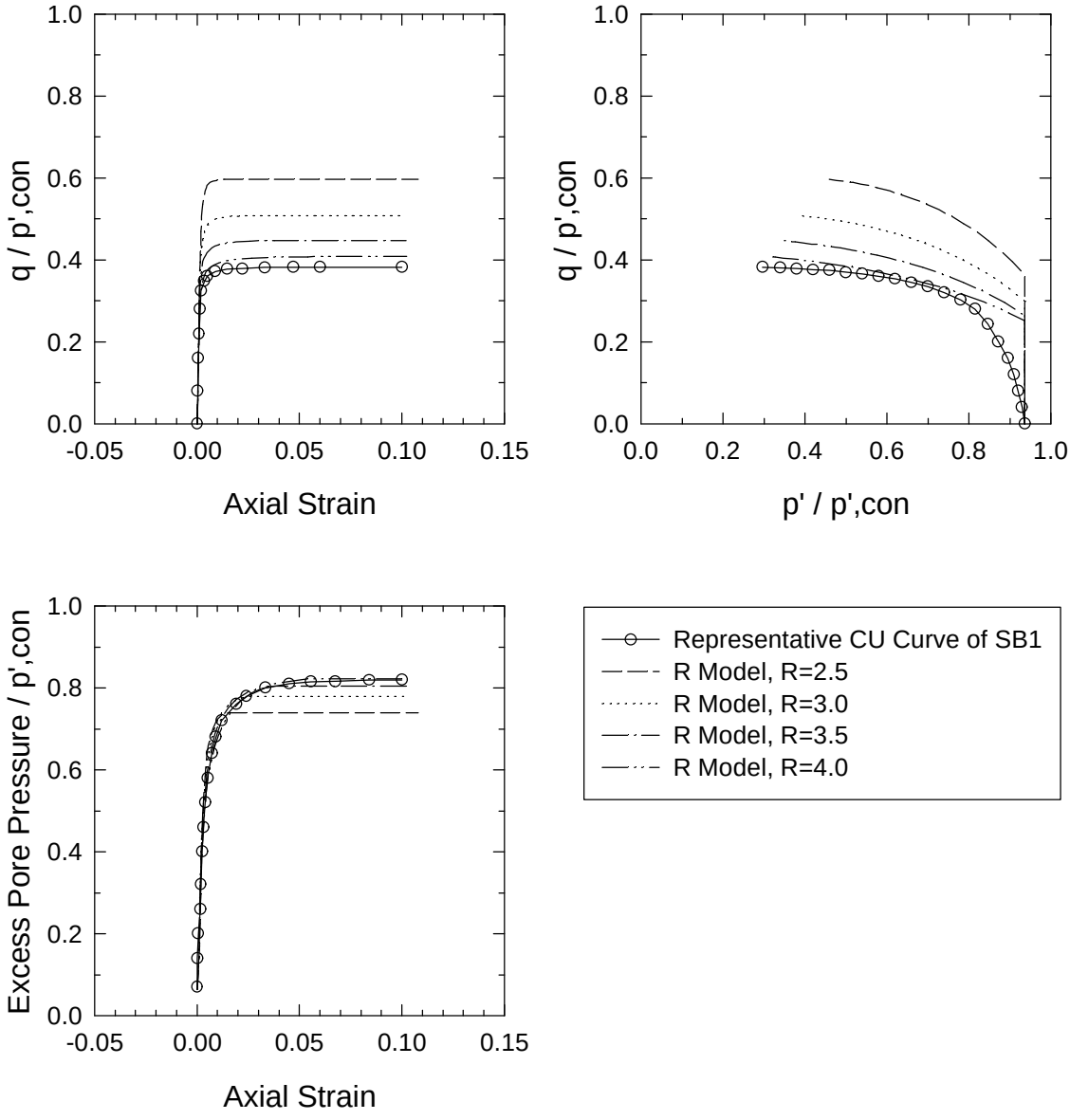

Figure 4.20 Representative Normalized CU Test of SB1 and R Model with Varying R Values

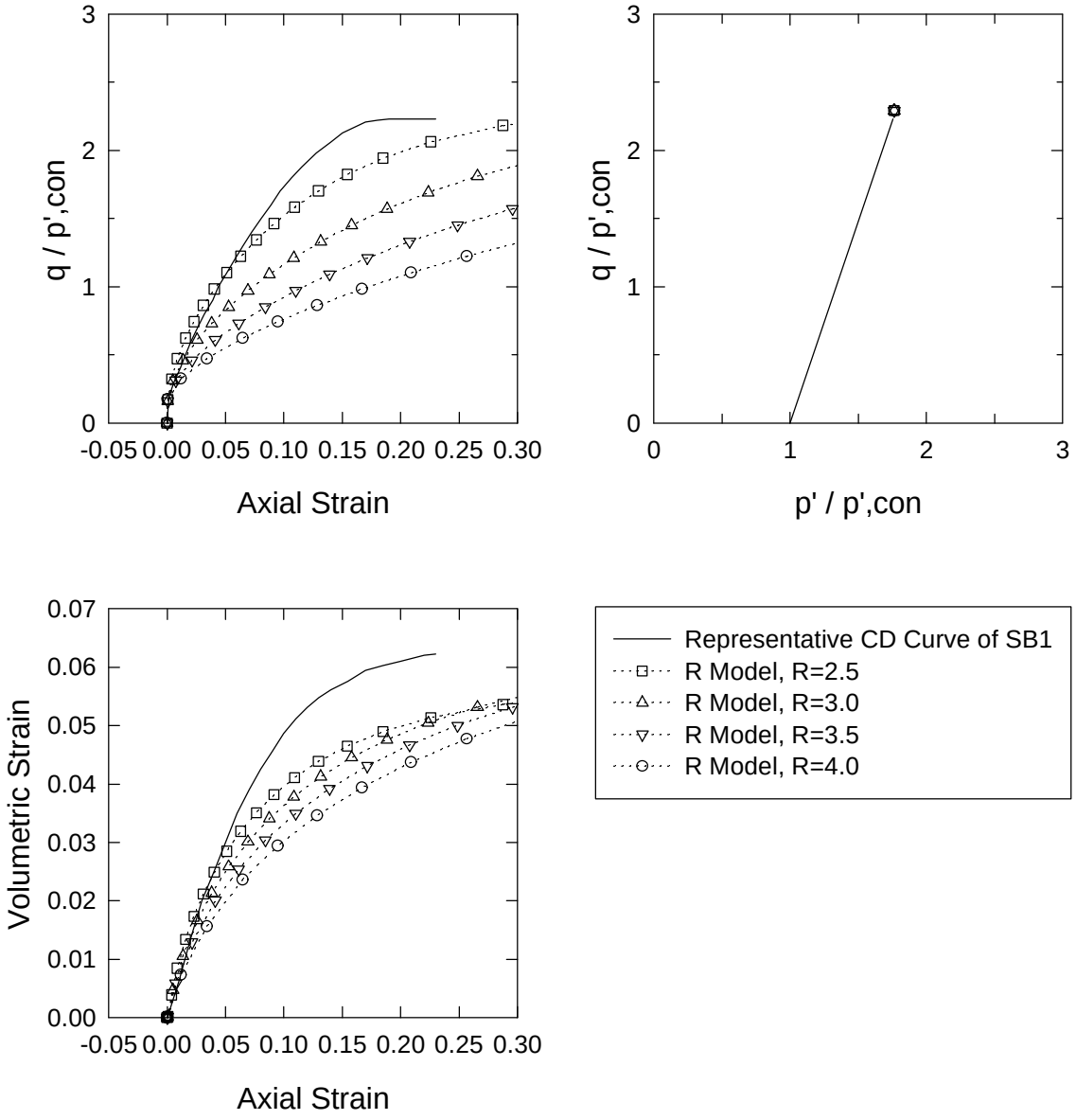

Figure 4.21 Representative Normalized CD Test of SB1 and R Model with Varying R Values

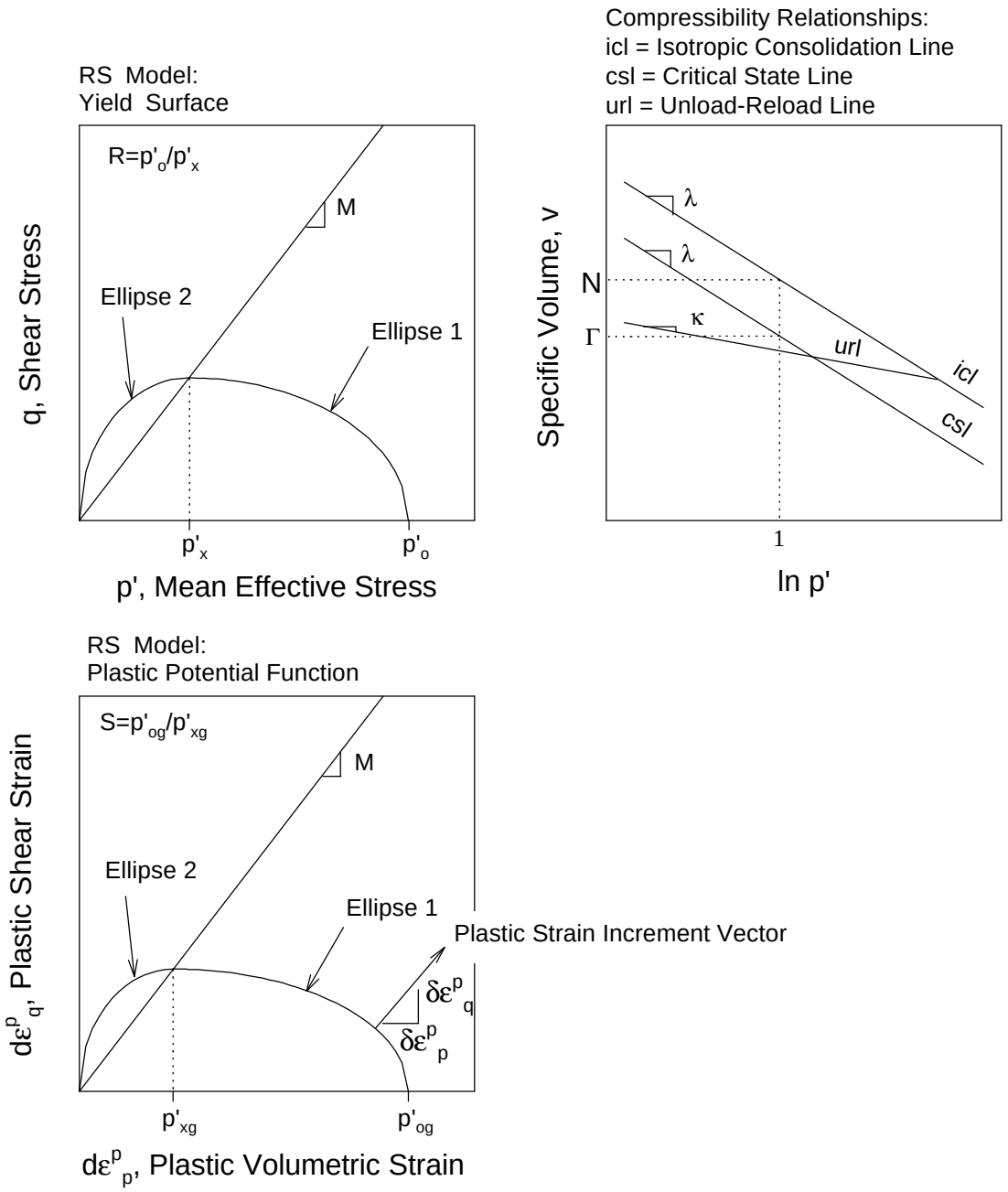

Figure 4.22 Properties of RS Model

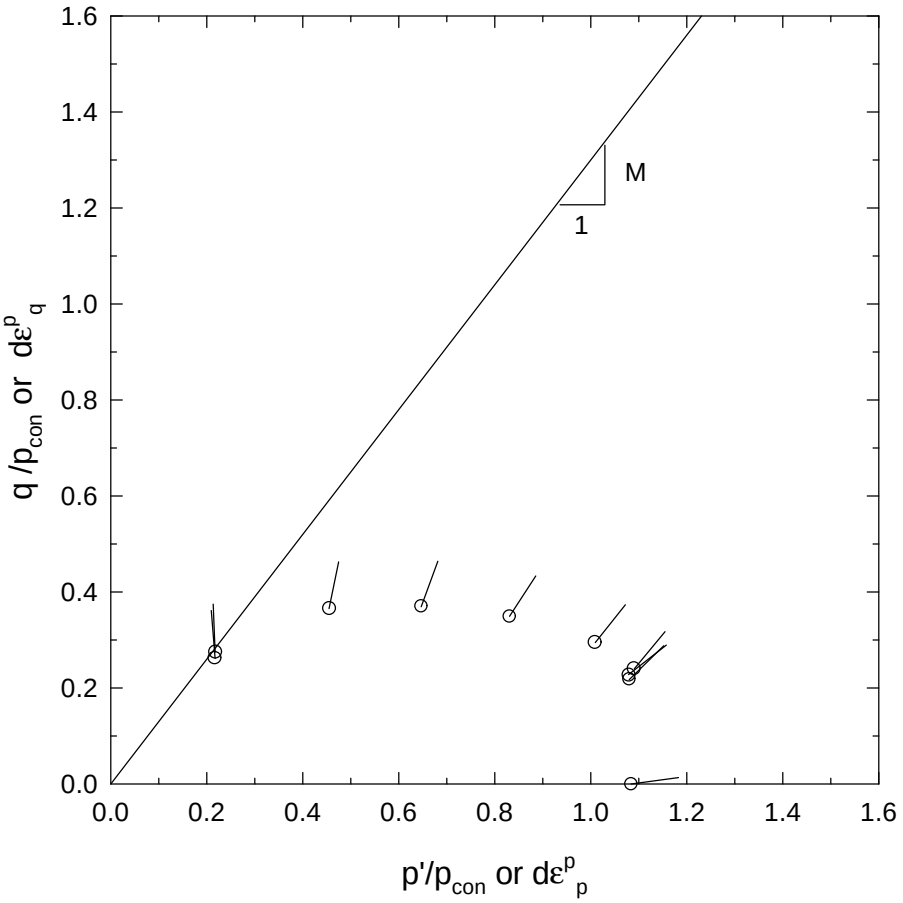

Figure 4.23 Plastic Strain Increment Vectors for SB1 Plotted at Yield Points

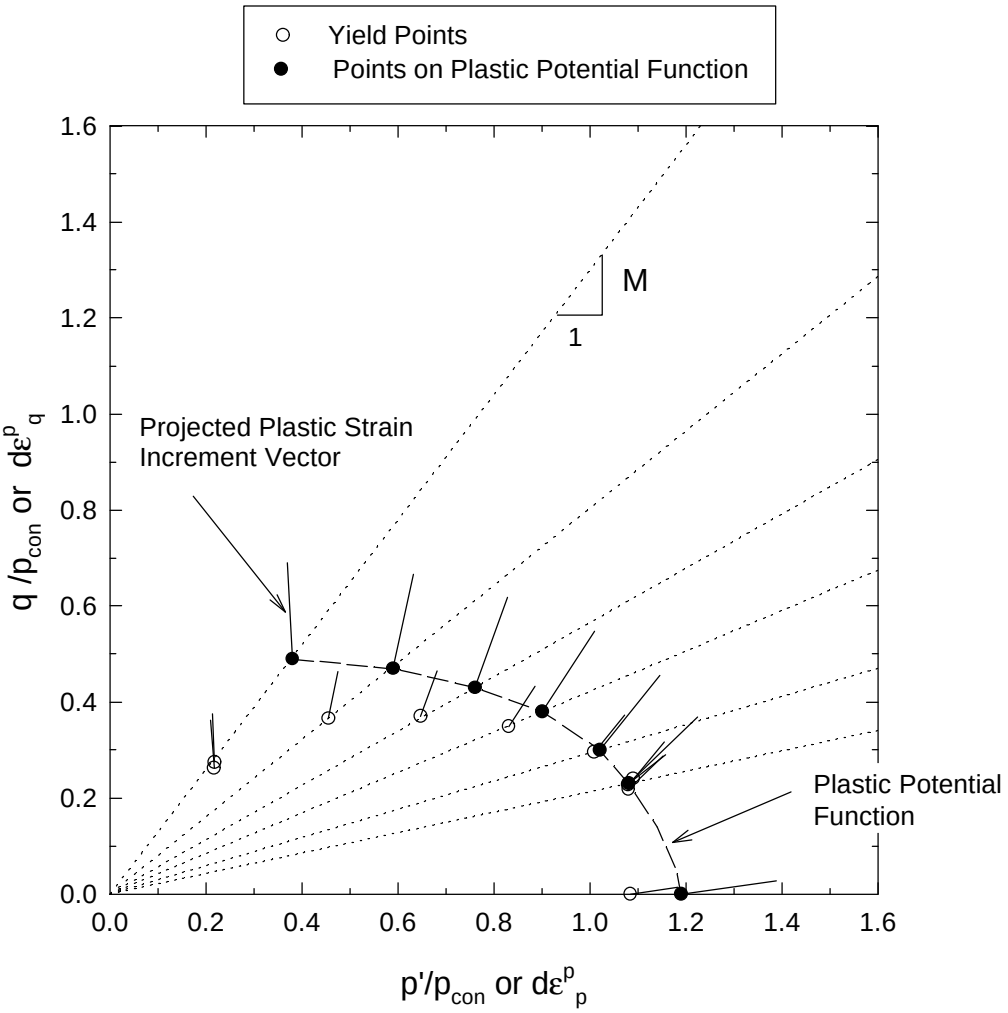

Figure 4.24 Estimated Shape of Plastic Potential Function for SB1

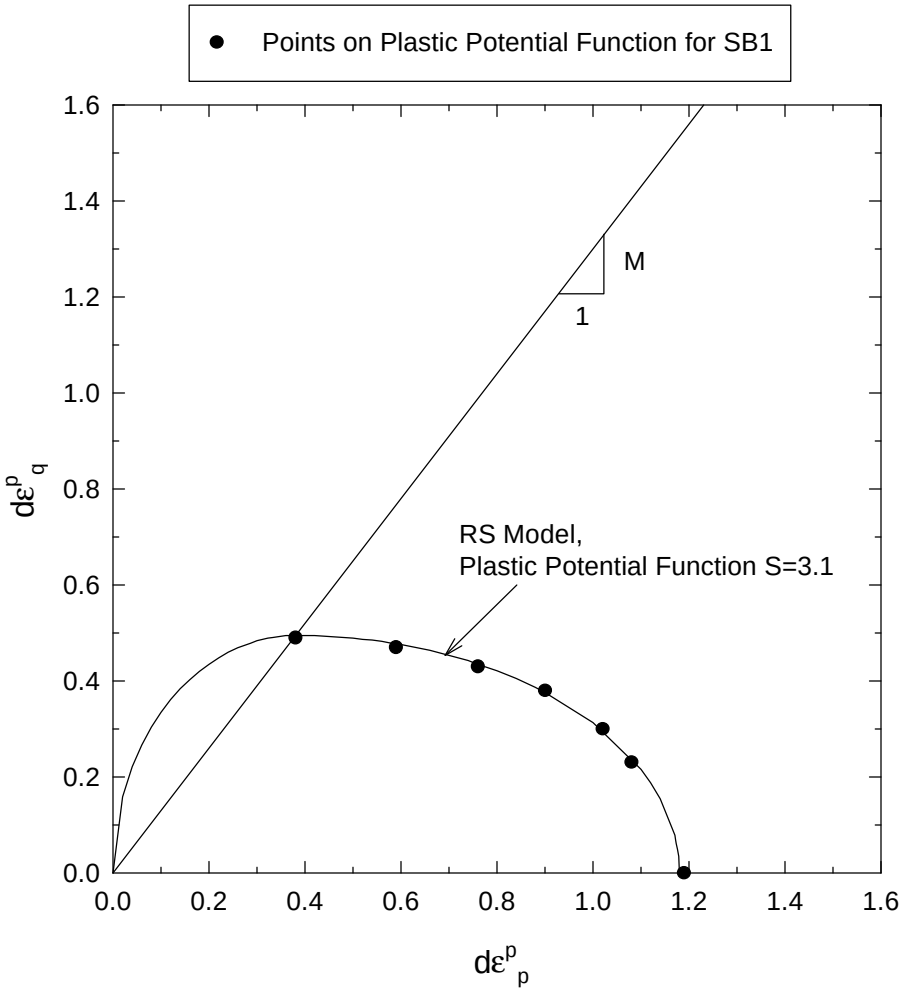

Figure 4.25 Points on Plastic Potential Function for SB1 and RS Model Plastic Potential Function with S=3.1

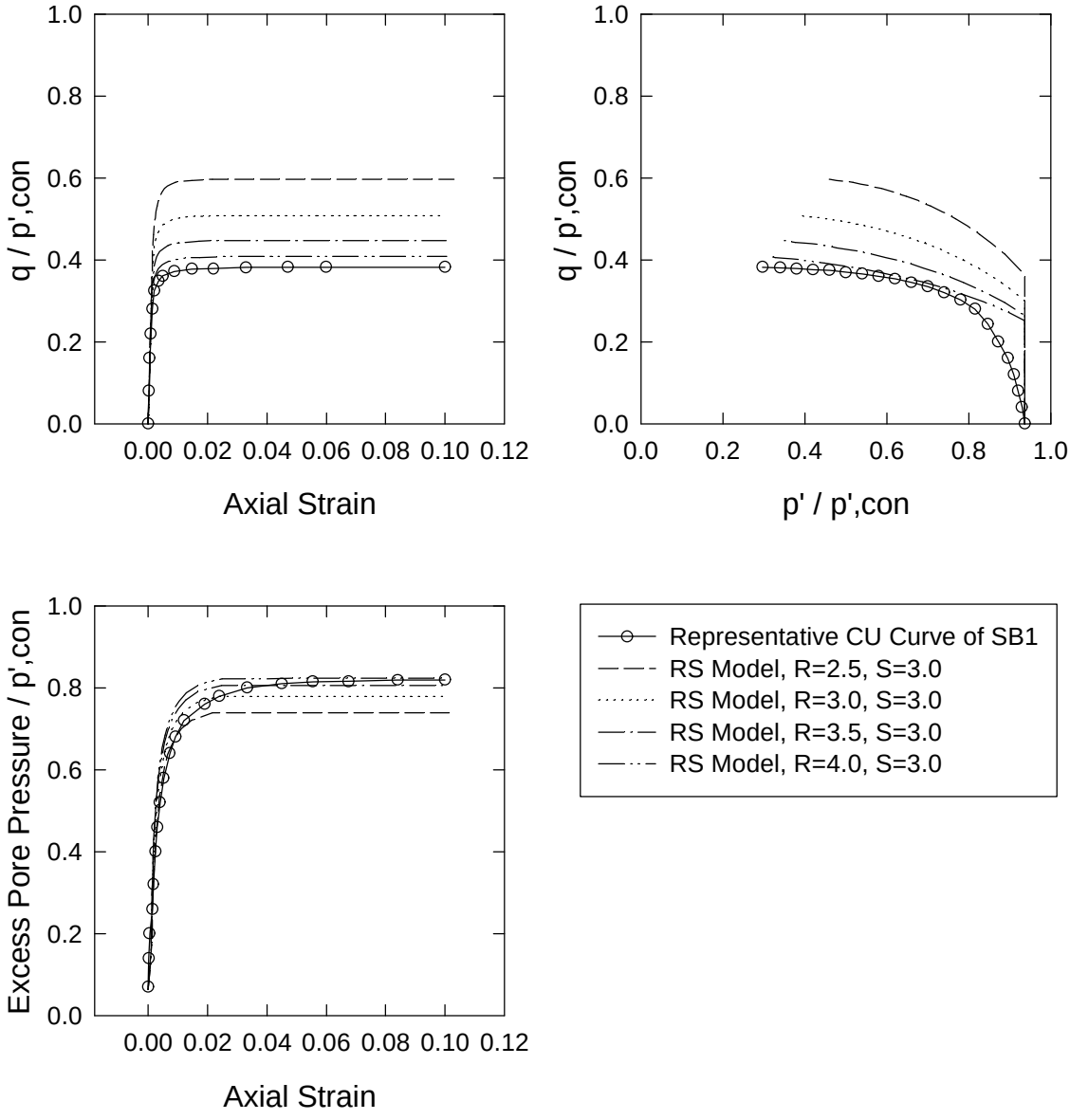

Figure 4.26 Representative Normalized CU Test of SB1 and RS Model with Varying R Values and Constant S Value

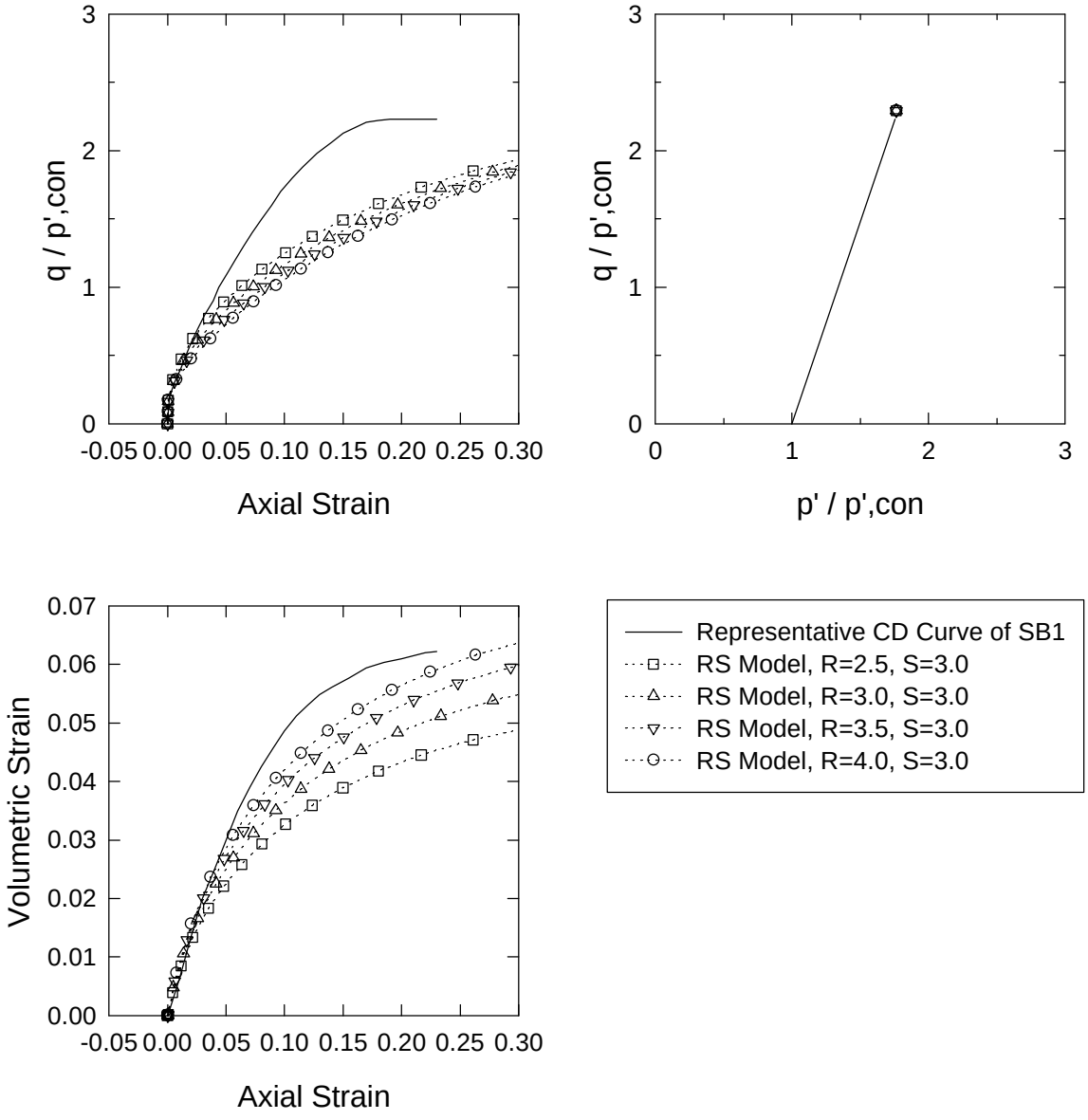

Figure 4.27 Representative Normalized CD Test of SB1 and RS Model with Varying R Values and Constant S Value

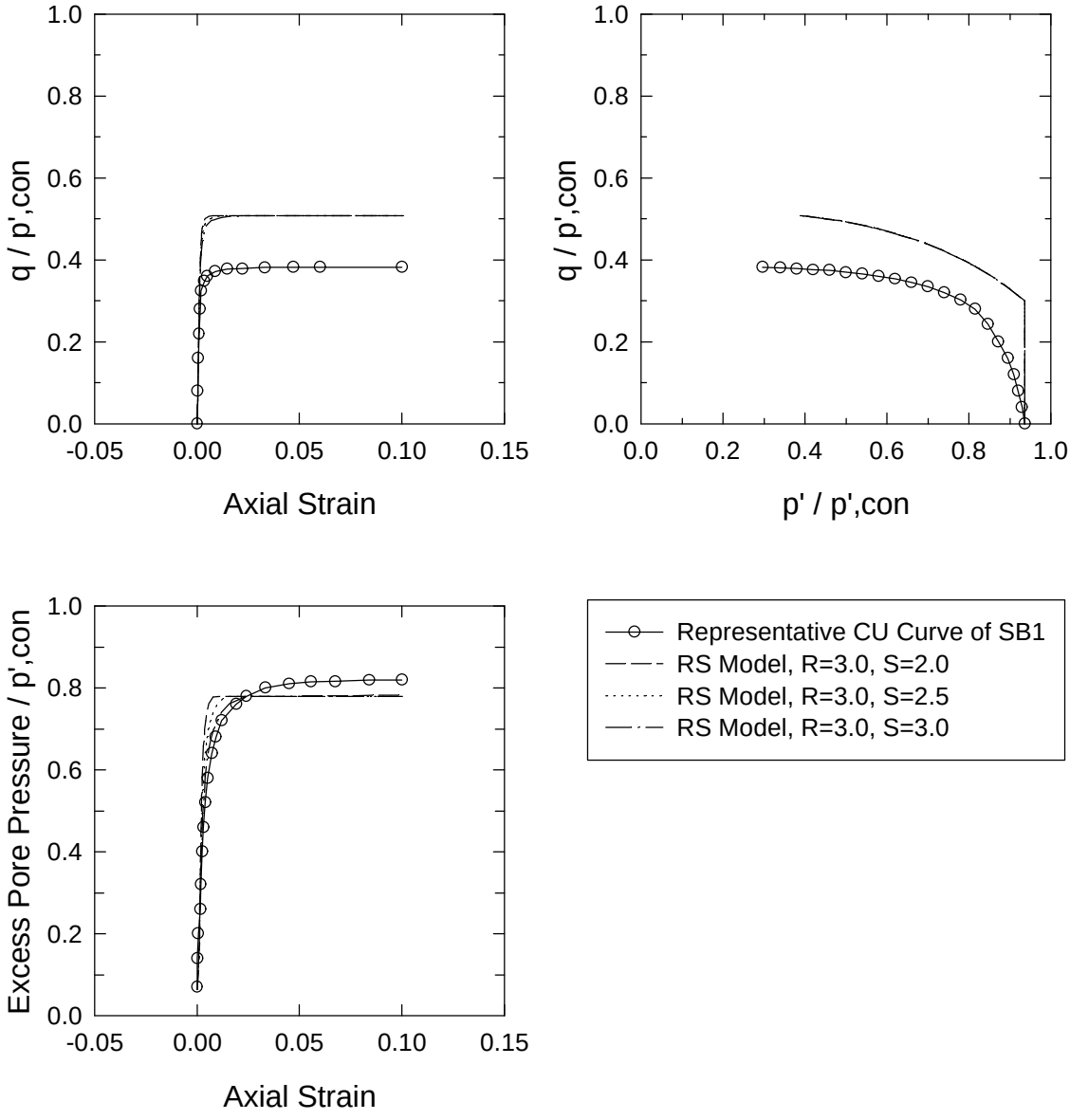

Figure 4.28 Representative Normalized CU Test of SB1 and RS Model with Varying S Values and Constant R Value

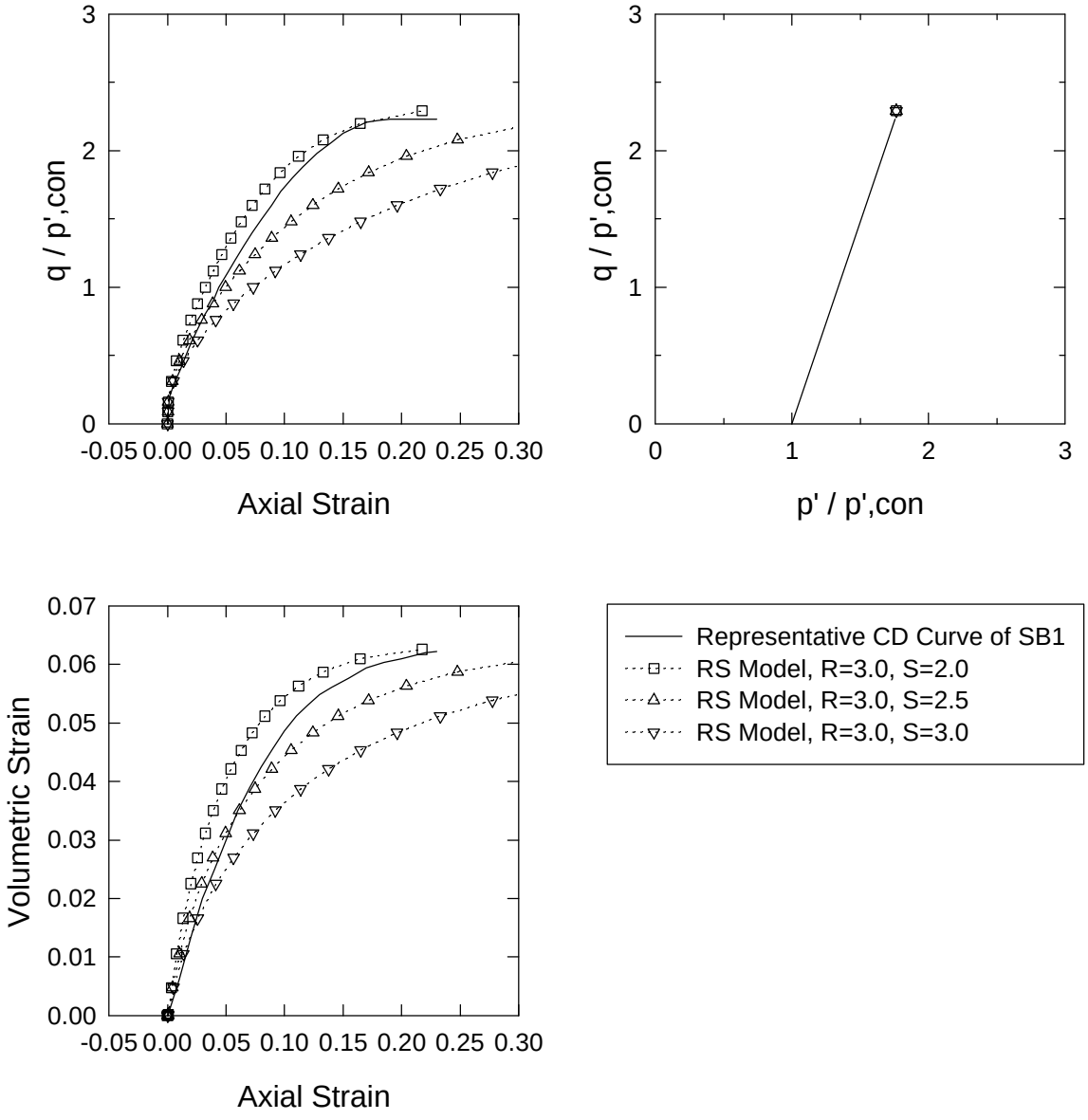

Figure 4.29 Representative Normalized CD Test of SB1 and RS Model with Varying S Values and Constant R Value

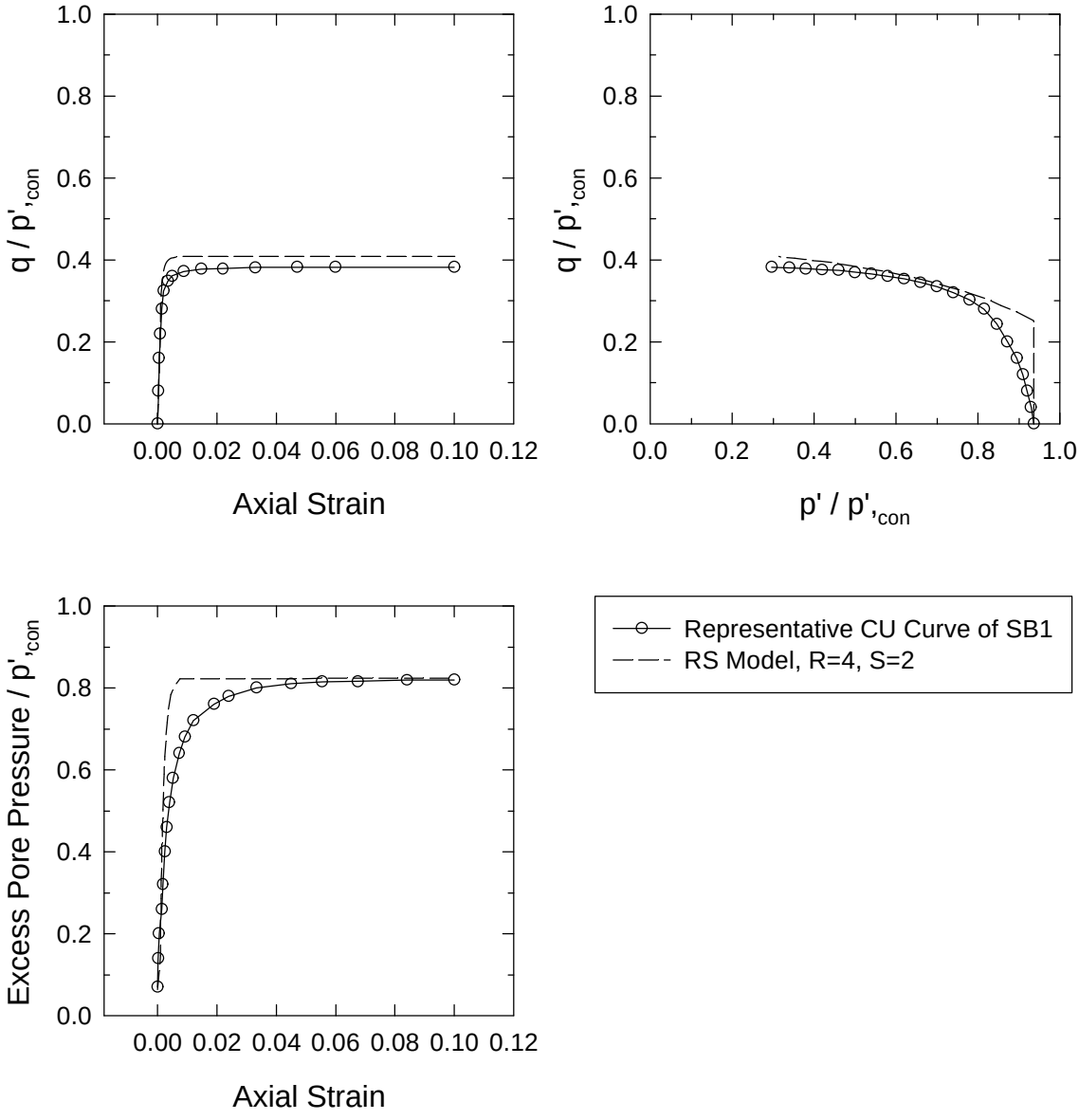

Figure 4.30 Representative Normalized CU Test of SB1 and RS Model with Best Fit R and S Parameters

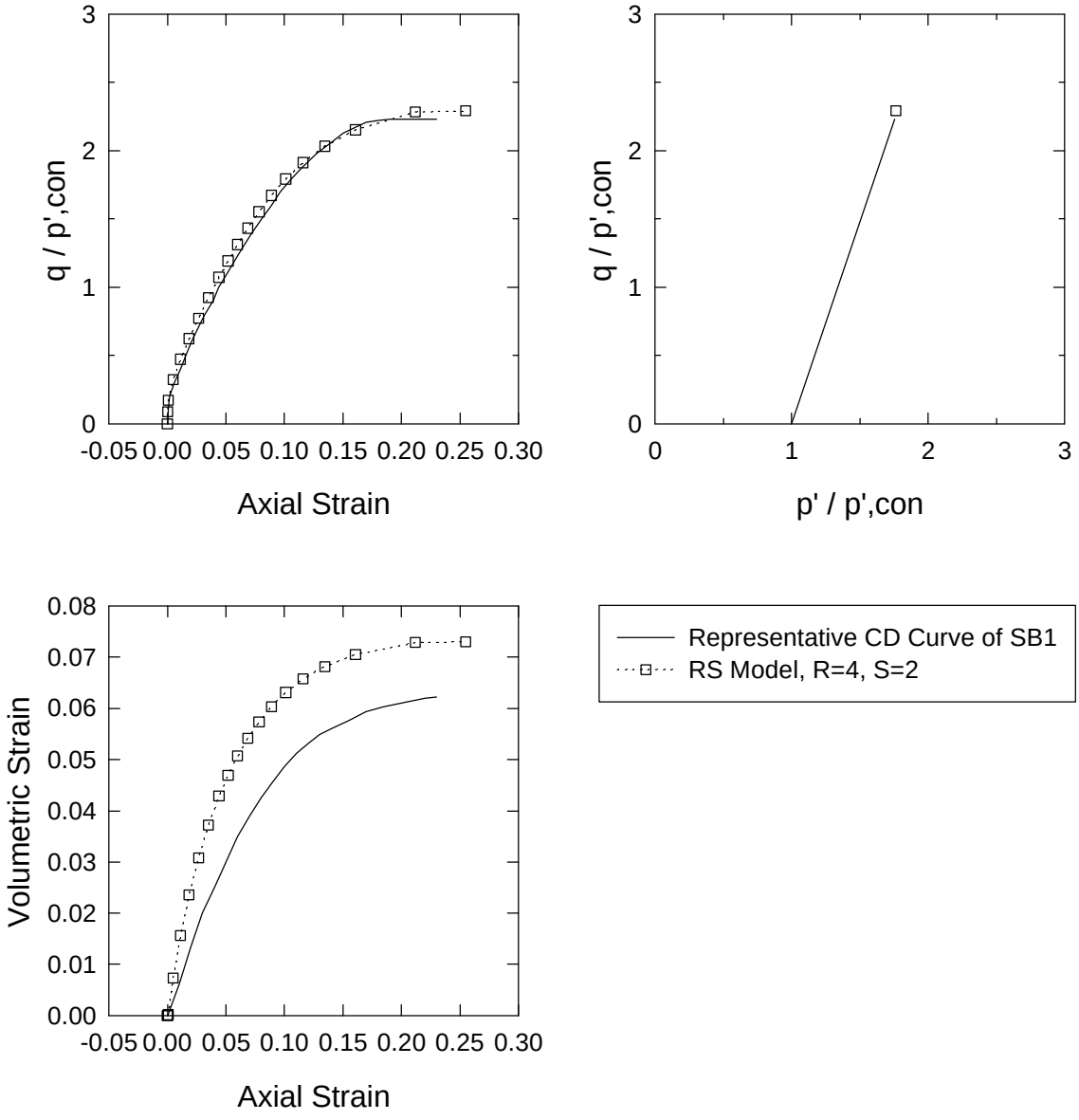

Figure 4.31 Representative Normalized CD Test of SB1 and RS Model with Best Fit R and S Parameters

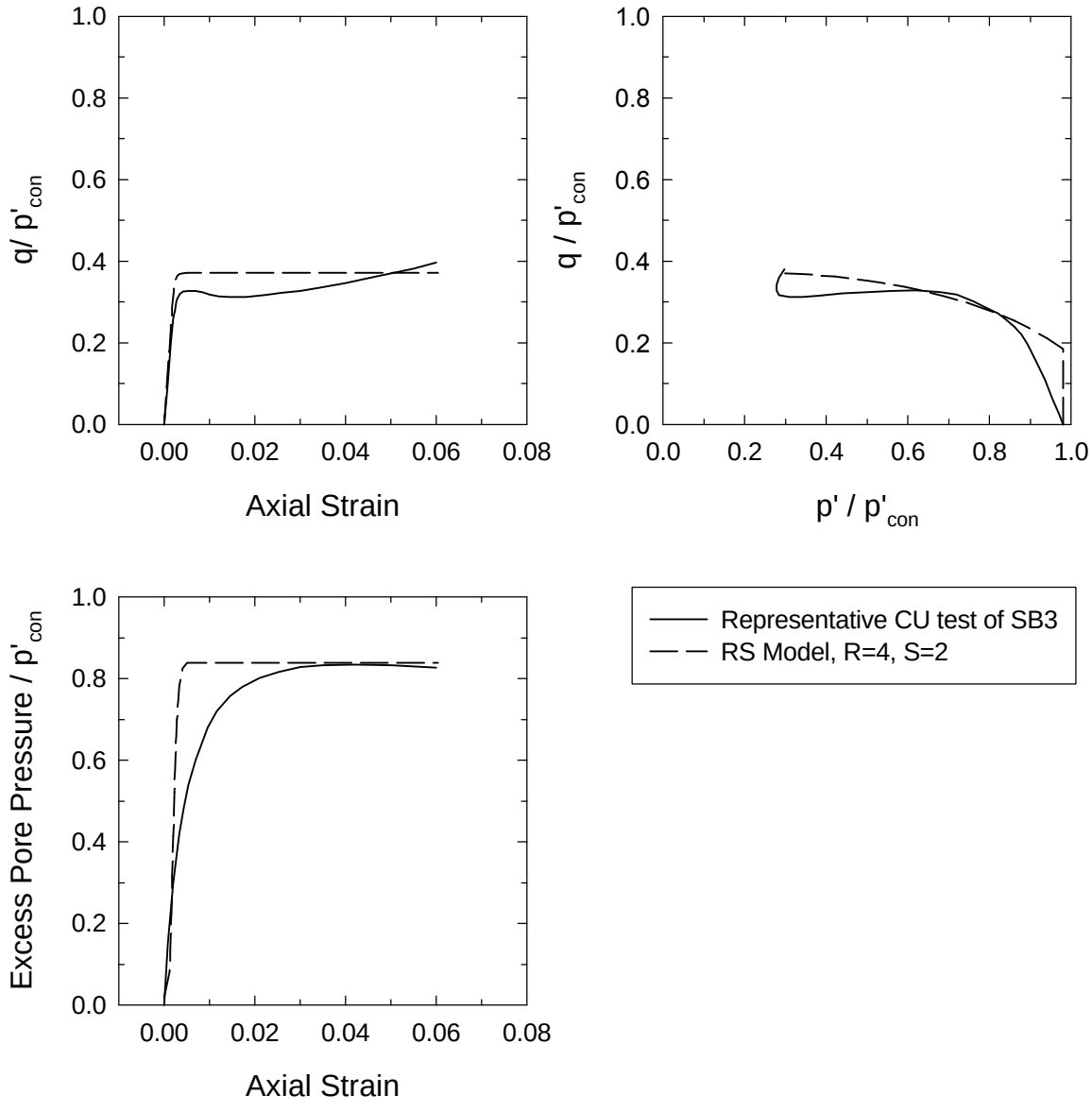

Figure 4.32 Representative Normalized CU Test of SB3 and RS Model with Best Fit R and S Parameters

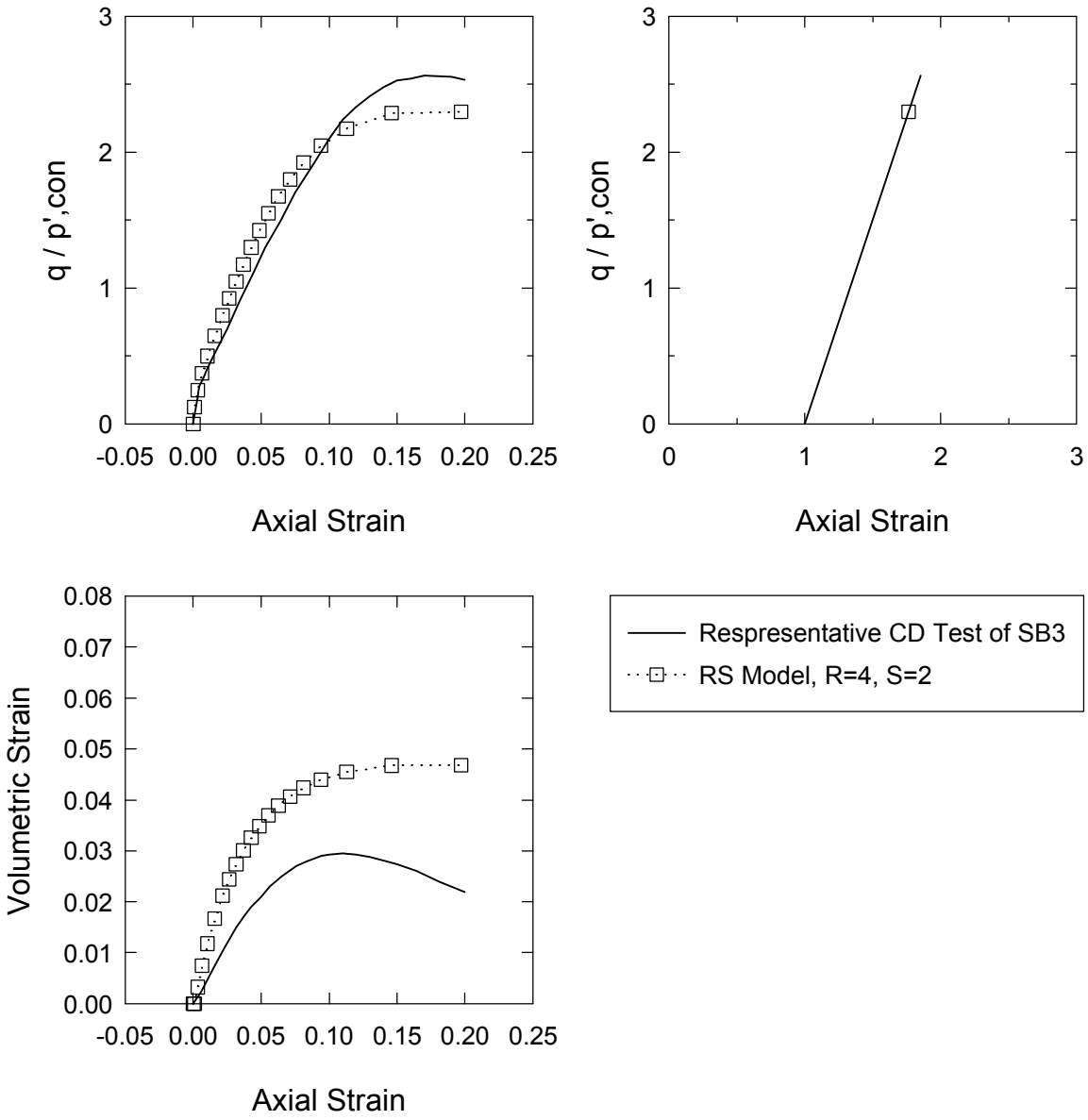

Figure 4.33 Representative Normalized CD Test of SB3 and RS Model with Best Fit R and S Parameters